Blockade of Vascular Endothelial Growth Factor Suppresses Experimental Restenosis After Intraluminal Injury by Inhibiting Recruitment of Monocyte Lineage Cells

Kisho Ohtani, MD; Kensuke Egashira, MD, PhD; Ken-ichi Hiasa, MD; Qingwei Zhao, MD; Shiro Kitamoto, MD; Minako Ishibashi, MD; Makoto Usui, MD; Shujiro Inoue, MD; Yoshikazu Yonemitsu, MD; Katsuo Sueishi, MD; Masataka Sata, MD; Masabumi Shibuya, MD; Kenji Sunagawa, MD

Background—Therapeutic angiogenesis by delivery of vascular endothelial growth factor (VEGF) has attracted attention. However, the role and function of VEGF in experimental restenosis (neointimal formation) after vascular intraluminal injury have not been addressed.

Methods and Results—We report herein that blockade of VEGF by soluble VEGF receptor 1 (*sFlt-1*) gene transfer attenuated neointimal formation after intraluminal injury in rabbits, rats, and mice. *sFlt-1* gene transfer markedly attenuated the early vascular inflammation and proliferation and later neointimal formation. *sFlt-1* gene transfer also inhibited increased expression of inflammatory factors such as monocyte chemoattractant protein-1 and VEGF. Intravascular VEGF gene transfer enhanced angiogenesis in the adventitia but did not reduce neointimal formation.

Conclusions—Increased expression and activity of VEGF are essential in the development of experimental restenosis after intraluminal injury by recruiting monocyte-lineage cells. (***Circulation.* 2004;110:2444-2452.)**

Key Words: restenosis ■ remodeling ■ inflammation ■ endothelium-derived factors ■ gene therapy

Vascular endothelial growth factor (VEGF) has attracted attention for endothelial regeneration and angiogenesis.[1–3] VEGF is one of the most potent vascular permeability factors known, is thought to function as an endogenous regulator of endothelial integrity after injury, and thus, protects the artery from disease progression.[4] Previous animals studies have reported that local delivery of VEGF after endothelial injury promotes endothelial regeneration, accelerates the recovery of endothelium-dependent relaxation, and reduces neointimal formation (see review[4]), suggesting the close correlation between accelerated endothelial integrity and reduced neointima after balloon injury. Increased expression of VEGF and its 2 receptors (VEGFR-1, Flt-1; VEFGR-2, Flk-1) in atherosclerotic and restenotic lesions has been reported.[5–7] However, there is still considerable debate over the vasculoprotective versus atherogenic effects of VEGF.[8] Emerging evidence suggests that (1) VEGF induces migration and activation of monocytes[9]; (2) VEGF induces adhesion molecules[10] and monocyte chemoattractant protein-1 (MCP-1)[11]; and (3) VEGF enhances neointimal formation and atherogenesis by stimulating intraplaque angiogenesis in hypercholesterolemic animals without balloon injury[12,13] or by increasing monocyte infiltration into atherosclerotic lesions.[14] Therefore, it remains unclear whether VEGF protects the artery from vascular disease or accelerates vascular disease.

See p 2283

Clinical and experimental studies involving arterial gene transfer of VEGF showed that it failed to reduce restenosis after balloon angioplasty.[15–17] The role of VEGF in restenotic changes (neointimal formation and negative remodeling) after injury therefore remains a mystery. This is mainly because the inhibitor of VEGF has not been tested for experimental restenosis, although inhibitors of VEGF are currently being evaluated for tumor angiogenesis and other treatment-intractable inflammatory disorders.[3] It is practically impossible to investigate the role of VEGF in postnatal life in mice lacking VEGF or its receptors, because the absence of VEGF function leads to embryonic lethality owing to vascular defects.[4] A soluble form of the VEGF receptor-1 (sFlt-1) is expressed endogenously by vascular endothelial cells and can inhibit VEGF activity by directly sequestering VEGF and by functioning as a dominant-negative inhibitor against VEGF.[18] We and others have demonstrated that intramuscular transfection of the *sFlt-1* gene effectively and specifically

Received June 18, 2004; revision received August 14, 2004; accepted August 20, 2004.

From the Departments of Cardiovascular Medicine (K.O., K.E., M.U., Q.Z., S.K., M.I., K.-i.H., S.I., K.S.) and Pathology (Y.Y., S.K.), Graduate School of Medical Sciences, Kyushu University, Fukuoka; the Department of Cardiovascular Medicine (M. Sata), Graduate School of Medical Sciences, University of Tokyo, Tokyo; and the Division of Genetics (M. Shibuya), Institute of Medical Science, University of Tokyo, Tokyo, Japan.

An online-only Data Supplement is available at http://www.circulationaha.org

Correspondence to Kensuke Egashira, MD, PhD, Department of Cardiovascular Medicine, Graduate School of Medical Science, Kyushu University, 3-1-1, Maidashi, Higashi-ku, Fukuoka 812-8582, Japan. E-mail egashira@cardiol.med.kyushu-u.ac.jp

© 2004 American Heart Association, Inc.

Circulation **is available at http://www.circulationaha.org** **DOI: 10.1161/01.CIR.0000145123.85083.66**

blocks VEGF and thus, "quenches" the activity of VEGF in remote organs in vivo.[19,20]

The aim of this study was to decisively determine a role for VEGF in restenotic changes after intraluminal injury. We report herein that blockade of VEGF by systemic *sFlt-1* gene transfer attenuates the development of neointimal formation after intraluminal injury by inhibiting inflammation, which suggests an essential role for VEGF in the pathogenesis of restenosis after injury. Our present data are clinically important because VEGF gene therapy for therapeutic angiogenesis and restenosis has been attempted in clinical studies.[16,17,21]

Methods

Expression Vector

The 3.3-kb mouse *sFLT-1* gene, originally obtained from the mouse lung DNA library,[22] was cloned into the *Bam*HI (5′) and *Not*1 (3′) sites of the eukaryotic expression vector plasmid cDNA3 (Invitrogen). Plasmid cDNA3 encoding the luciferase gene was used to detect gene transfection.

Rat and Rabbit Models of Balloon Injury

The study protocol was reviewed and approved by the Committee on Ethics on Animal Experiments, Kyushu University Faculty of Medicine, and the experiments were conducted according to the guidelines of American Physiological Society. A portion of this study was performed at the Kyushu University Station for Collaborative Research.

Twenty-week-old male, normal chow–fed Wistar-Kyoto rats were anesthetized, and their right common carotid arteries were injured by passage (3 times) of an infiltrated 2F Fogarty balloon catheter.[23] Male Japanese white rabbits weighing 3.0 to 3.5 kg were fed a high-cholesterol diet for 2 weeks. Their right common carotid arteries also were injured by passage (3 times) of an inflated 2F Fogarty catheter.[24] After injury, all rabbits were fed the same high-cholesterol diet. Three days before balloon injury, the animals were randomly divided into 2 groups: the empty-plasmid group was injected with the empty plasmid, and the *sFlt-1* group was injected with the *sFlt-1* gene into femoral muscle (150 μg/50 μL TE buffer [10 mmol/L Tris-HCl, 1 mmol/L EDTA, pH 8.0] in rats, 1500 μg/0.5 mL TE buffer in rabbits). To enhance transgene expression, all plasmid-injected animals received electroporation at the injection site immediately after injection with an electric pulse generator (CUY21, BTX) as previously described.[19,23–25]

Morphometric and Immunohistochemical Analyses

All animals were euthanized by intravenous injection of a lethal dose of sodium pentobarbital. Tissue sections from rabbits and rats were prepared as described[23,24] and either (1) stained with Masson's trichrome or elastica van Gieson's stains or (2) subjected to immunostaining with antibodies against macrophages/monocytes (ED1, Serotec, for rats; RAM11, Dako, for rabbits), proliferating cells (proliferating cell nuclear antigen for rats from Dako, Ki-67 for rabbits from Dako), endothelial cells (CD31, Dako), VEGF (Santa Cruz), VEGFR-1 (Santa Cruz), VEGFR-2 (Santa Cruz), α-smooth muscle actin (Dako), MCP-1 (R&D Systems), interleukin-1β (IL-1β; R&D Systems), or nonimmune mouse IgG (Zymed). After avidin-biotin amplification, the slides were incubated with diaminobenzidine and counterstained with hematoxylin. Immunofluorescence double staining was performed to localize VEGF and its receptors by the use of fluorescence-conjugated antibodies in rats. Morphometric analysis was performed by microscopy with a computerized digital image-analysis system by a single observer who was blinded to the treatment protocol.[23,24]

Real-Time Quantitative Reverse Transcription–PCR

Real-time polymerase chain reaction (PCR) amplification was performed with rabbit cDNA by using the ABI PRISM 7000 sequence detection system (Applied Biosystems) as described previously.[23] The respective PCR primers and TaqMan probes were designed from GenBank databases aided by a software program (Applied Biosystems; online Table I). Results were analyzed by sequence detection software (Applied Biosystems), expressed in arbitrary units, and adjusted for glyceraldehyde 3-phosphate dehydrogenase mRNA levels.

Mouse Femoral Wire-Injury Model With Bone Marrow Reconstitution

Intraluminal injury of the femoral artery of wild-type mice whose bone marrow had been replaced with that of ROSA26 mice, which expresses β-galactosidase (LacZ) ubiquitously, was performed.[26] Four weeks after bone marrow transplantation, transluminal arterial injury was induced by inserting a straight spring wire (0.38 mm in diameter) into the femoral artery as described.[26] The femoral artery was excised and stained with X-gal solution for 7 hours and then fixed in 4% paraformaldehyde. LacZ-positive cells were counted and expressed as a proportion of the total number of cells. The paraffin-embedded sections were stained with elastica van Gieson's stain.

Peripheral blood was obtained from the retro-orbital venous plexus of the mice. Fluorescence-conjugated antibodies against CD31 (Pharmingen) and c-Kit (Pharmingen) were used as bone marrow–derived monocyte-lineage markers. A fluorescein isothiocyanate–conjugated antibody against Mac-1 (Pharmingen) was used as a circulating monocyte-lineage marker after gating for monocyte cell size with exclusion of granulocytes. Data were analyzed by flow cytometry and appropriate software (Becton Dickinson).

Blood Measurements

Plasma total cholesterol levels in rabbits were determined with commercially available kits (Wako Pure Chemicals). To measure sFlt-1 released by the transfected skeletal muscle, plasma concentrations of sFlt-1 were measured by use of an sFlt-1 ELISA kit (R&D Systems) in rabbits. Concentrations of VEGF in plasma and femoral arterial tissues were also measured in mice by use of an ELISA kit (R&D Systems).

Statistical Analysis

Data are expressed as mean±SE. Statistical analysis of differences was compared by ANOVA and Bonferroni's multiple-comparison tests. A level of $P<0.05$ was considered statistically significant.

Results

Increased Expression of VEGF and Its Receptors in Rabbits and Rats

Significant increases in VEGF mRNA levels were detected after balloon injury in rabbits, which peaked on day 7 and persisted until day 28 (Figure 1A). Immunohistochemical staining revealed that VEGF and VEGFR-1 increased in vascular smooth muscle cells in the media and regenerated endothelial layer during the early phase (day 7) and in cells in the neointima, media, and adventitia during the later phase (day 28) after balloon injury in rabbits (Figure 1B). VEGFR-2 did not increase on day 7 but did increase in the injured artery on day 28. *sFlt-1* gene transfer reduced the increased immunoreactivities of VEGF, VEGFR-1, and VEGFR-2 on day 28 (Figure 1B).

The localization of VEGF, VEGFR-1, and VEGFR-2 was studied in rats by immunohistochemistry. As observed in rabbits, immunoreactive VEGF and VEGFR-1 increased in the media on days 3 and 7 and in the neointima, media, and adventitia on day 28 (Figure 2A). The increase in immunoreactive VEGFR-2 was less prominent during the early phase but became apparent on day 28 (Figure 2A).

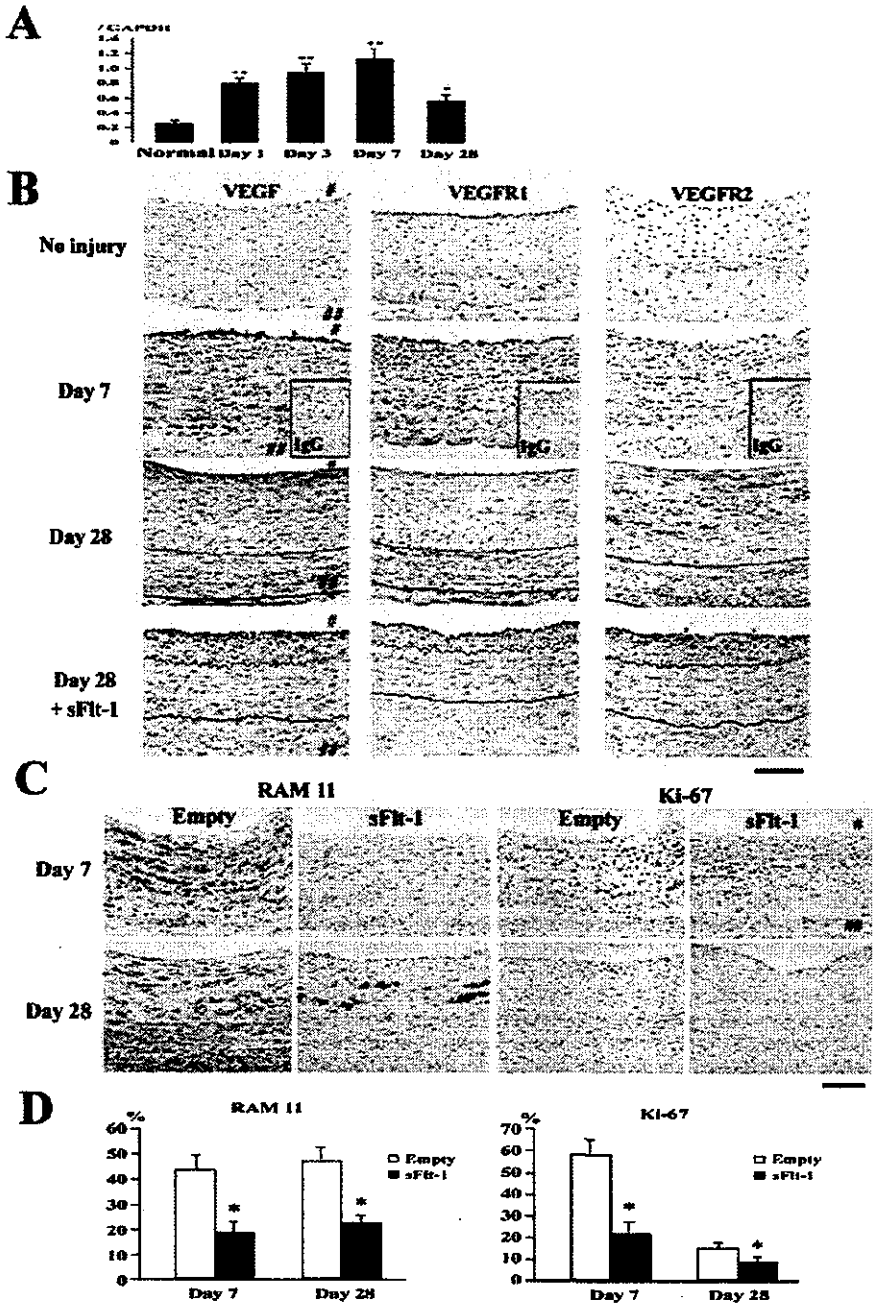

Figure 1. Expression of VEGF after balloon injury and inhibitory effects of *sFlt-1* gene transfer on inflammatory-proliferative changes in rabbits. A, Time course of VEGF mRNA levels in rabbits. mRNA levels were assessed by real-time PCR at indicated times. Expression of VEGF mRNA in each sample was normalized to glyceraldehyde 3-phosphate dehydrogenase mRNA expression in that sample. Each bar has n=6 to 8. *$P<0.05$, **$P<0.01$ vs control (uninjured) artery. B, Immunohistochemistry of rabbit carotid artery. Arterial cross sections were stained immunohistochemically with VEGF, VEGFR-1 (Flt-1), VEGFR-2 (Flk-1), or nonimmune IgG. # and ## indicate lumen and adventitia, respectively. Internal and external elastic layers are highlighted with blue and black lines, respectively, in photographs taken 28 days after injury. Bar indicates 100 μm. C, Carotid artery sections from empty-plasmid and *sFlt-1* groups 7 and 28 days after balloon injury were stained immunohistochemically with antibody against monocytes/macrophages (RAM11) or proliferating cells (Ki-67). # and ## indicate lumen and adventitia, respectively. Bar=100 μm. D, Effect of *sFlt-1* gene transfer on inflammation (RAM11-positive monocytes/macrophages) and proliferation (Ki-67–positive cells) 7 and 28 days after balloon injury (*n=8 each*). *$P<0.01$ vs control group.

Fluorescence double immunohistochemistry revealed that VEGF and VEGFR-1 were expressed predominantly in α-smooth muscle actin–positive cells in the media and neointima on day 28 (Figure 2B). During the early phase, ED1-positive monocytes recruited into the intima and adventitia expressed VEGFR-1 but not VEGFR-2 (Figure 2C). *sFlt-1* gene transfer reduced the increased immunoreactivities of VEGF, VEGFR-1, and VEGFR-2 on day 28 (data not shown).

Inhibitory Effects of *sFlt-1* Transfer on Inflammatory and Proliferative Changes in Rabbits

As we reported,[23,24] inflammatory and proliferative changes became evident by 3, 7, and 28 days after balloon injury in rabbits (Figure 1C and 1D). *sFlt-1* gene transfer reduced these inflammatory and proliferating changes.

Inhibitory Effects of *sFlt-1* Transfer on Neointimal Formation and/or Negative Remodeling in Rabbits and Rats

The carotid arteries in the control and empty-plasmid groups developed significant neointimal formation and negative remodeling (smaller lumen size, internal elastic lamina, and external elastic lamina) in rabbits by day 28 (Figure 3A and 3B). The arteries from the *sFlt-1* group showed less neointimal formation, negative remodeling, perivascular fibrosis, and adventitial vasa vasorum; an adventitial VEGFR-2–positive vasa vasorum; and a larger lumen area. There was no significant difference in plasma levels of total cholesterol between the 2 groups (online Table II), indicating that the observed effects of *sFlt-1* gene transfer were not caused by changes in serum cholesterol levels. In rats, neointimal

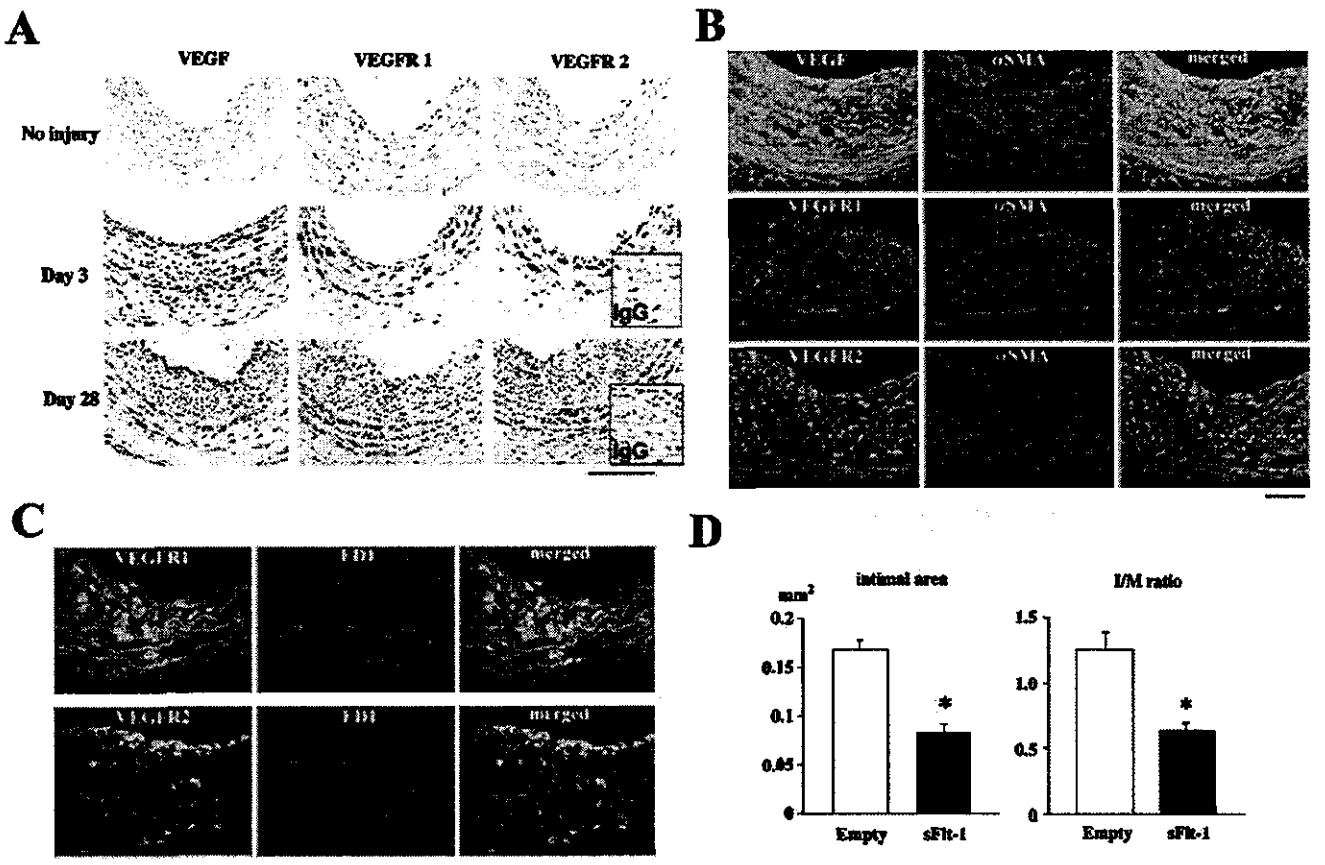

Figure 2. Expression of VEGF and its receptors after balloon injury and inhibitory effects of *sFlt-1* gene transfer on neointimal formation in rats. A, Immunohistochemistry of arterial cross-sections stained immunohistochemically with VEGF, VEGFR-1 (Flt-1), or VEGFR-2 (Flk-1). Bar indicates 100 μm. B, Fluorescence double immunohistochemistry 28 days after balloon injury. Photomicrographs show injured arteries stained with VEGF, VEGF-R1 (Flt-1), or VRGFR-2 (Flk-1) in green. Photomicrographs show injured arteries also stained with α-smooth muscle actin in red. Single-fluorescence–positive cells were stained in green or red, whereas double-positive cells were stained in yellow. Scale bar indicates 100 μm. C, Fluorescence double immunohistochemistry 7 days after balloon injury. Photomicrographs show injured arteries stained with VEGF-R1 or VEGF-R2 in green. Photomicrographs show injured arteries also stained with ED1 in red. Single-fluorescence–positive cells were stained in green or red, whereas double-positive cells were stained in yellow. Scale bar indicates 100 μm. D, Neointimal formation (neointimal area and intima-media ratio) on 28 day after balloon injury. *P<0.01 vs empty-plasmid group, n=8 or 9.

formation was also less in the *sFlt-1* group than in the empty-plasmid group on day 28 (Figure 2D).

To assess transfection efficacy of *sFlt-1*, plasma sFlt-1 concentration was measured in rabbits. The plasma sFlt-1 levels were 96±14, 377±25 (P<0.01 versus before), 413±20 (P<0.01), 284±15 (P<0.05), and 113±16 (P>0.1) pg/mL before and at 3, 7, 14, and 28 days after *sFlt-1* transfection, respectively, indicating that sFlt-1 was released from the transfected muscle to the circulation.

No Significant Effects of *sFlt-1* Gene Transfer on Endothelial Regeneration in Rabbits and Mice

In rabbits, there were no significant differences between the empty-plasmid and *sFlt-1*–transfected groups in the ratio of luminal surface area covered with endothelium (Figure 4A) and that of the CD31-positive endothelial layer 7 days after injury (Figure 4B). In mice, endothelial recovery was scarcely observed on day 7 (data not shown) but was noted equally in the 2 groups on day 14 (Figure 4C).

Inhibitory Effects of *sFlt-1* Transfer on Expression of Proinflammatory Factors

sFlt-1 transfection reduced the increased gene expression of MCP-1, platelet-derived growth factor, transforming growth factor-β, IL-1β, IL-6, tumor necrosis factor-α, matrix metalloproteinase-9, and VEGF (Figure 5A). *sFlt-1* transfer did not affect the increased gene expression of matrix metalloproteinase-1 and tissue factor. Immunohistochemical staining performed 7 days after balloon injury revealed increased immunoreactive MCP-1 and IL-1β in cells in the neointima and smooth muscle cells in the media, which were attenuated by *sFlt-1* gene transfer (Figure 5B).

Contribution of Bone Marrow Cells to the Effect of *sFlt-1* Gene Transfer in Mice

As reported,[26] a considerable proportion of neointimal and medial cells were LacZ-positive 28 days after injury in mice whose bone marrow expressed LacZ ubiquitously. Intimal area, intima-media ratio, and LacZ-positive cells were decreased in *sFlt-1*–transfected mice than in empty plasmid–

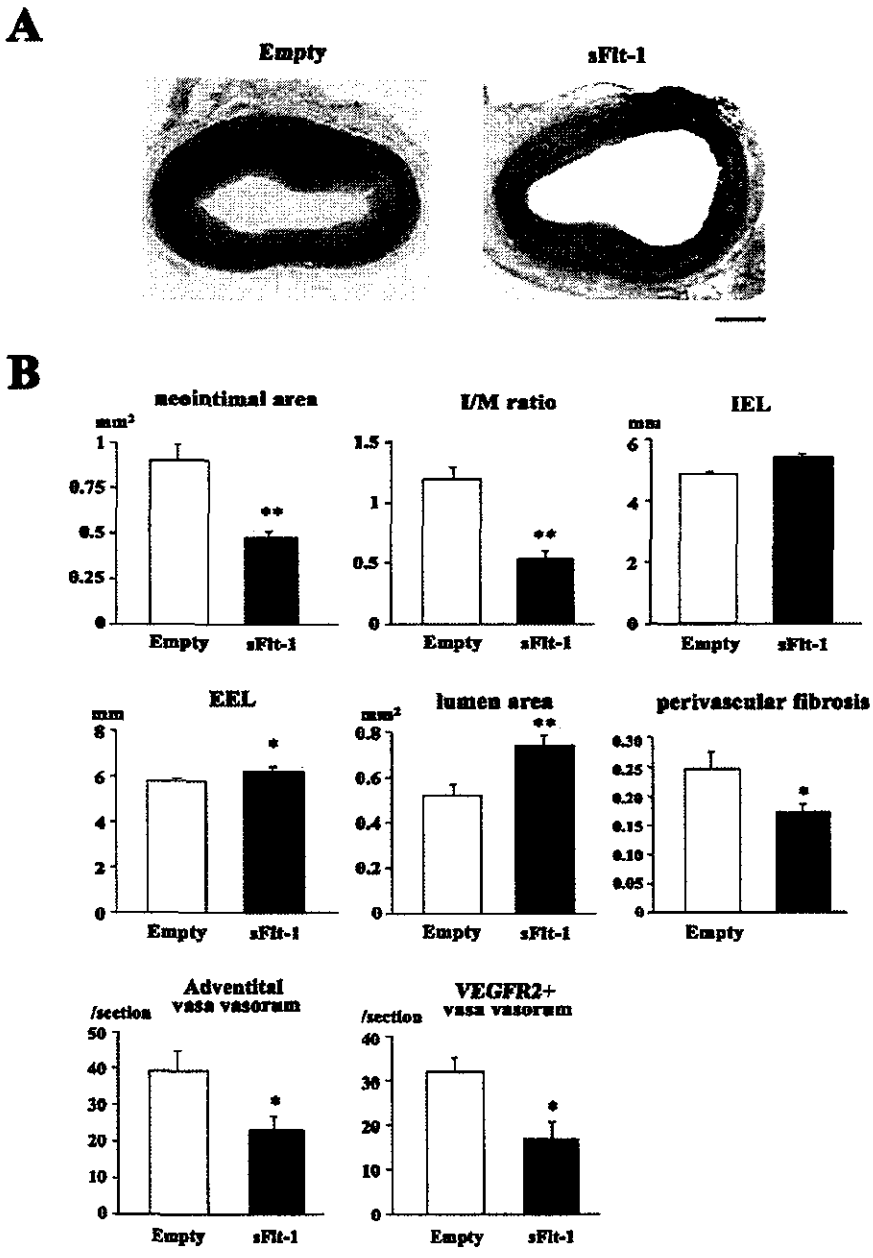

Figure 3. Inhibitory effect of *sFlt-1* gene transfer on restenotic changes (neointimal formation and negative remodeling) in rabbits. A, Carotid artery sections from empty-plasmid and *sFlt-1* groups 28 days after balloon injury stained with *elastica* van Gieson's stain. Bar=200 μm. B, Neointimal formation (neointimal area and intima-media ratio), negative remodeling (length of internal elastic lamina, length of external elastic lamina, and lumen area), perivascular fibrosis, adventitial vasa vasorum (number of CD31-positive vessels in adventitia), and VEGFR-2–positive vasa vasorum (number of VEGFR-2–positive vessels in adventitia) on day 28 after balloon injury are shown. *$P<0.05$, **$P<0.01$ vs empty-plasmid group, n=8 or 9.

transfected mice (Figure 6A and 6B). Wire injury also increased recruitment of bone marrow–derived monocytes (CD31-positive and c-Kit–positive) and circulating monocytes (Mac-1–positive) into peripheral blood (Figure 6C). *sFlt-1* gene transfer attenuated such changes in cell distribution, suggesting that wire injury increased such cell lineages in peripheral blood through VEGF. Plasma and femoral arterial concentrations of VEGF increased after wire injury, which was partly attenuated by *sFlt-1* transfection (online Tables III and IV).

Effects of $VEGF_{165}$ Gene Transfer on Neointimal Formation and Adventitial Angiogenesis in Rabbits

A recombinant adenoviral vector containing human $VEGF_{165}$ or the *LacZ* gene was produced. Gene transfer was performed by administering adenovirus solution (1 mL, 2×10^9 plaque-forming units) by a channel balloon catheter (Remedy, Boston Scientific Inc) immediately after balloon injury of rabbit carotid arteries (online Data Supplement and Figure). There were no significant differences between the empty-plasmid and *VEGF*-transfected groups in terms of neointimal formation, perivascular fibrosis, and negative remodeling (smaller lumen size, internal elastic lamina, and external elastic lamina) on day 28. In contrast, the number of adventitial vasa vasorum (the degrees of adventitial angiogenesis) was markedly increased in the *VEGF*-transfected group.

Discussion

VEGF has conventionally been thought to be an endothelial cell–specific growth factor and that it inhibits vascular pathological processes by accelerating endothelial proliferation and regeneration through endothelial VEGFR-2. If so, blockade of VEGF would suppress endothelial regeneration

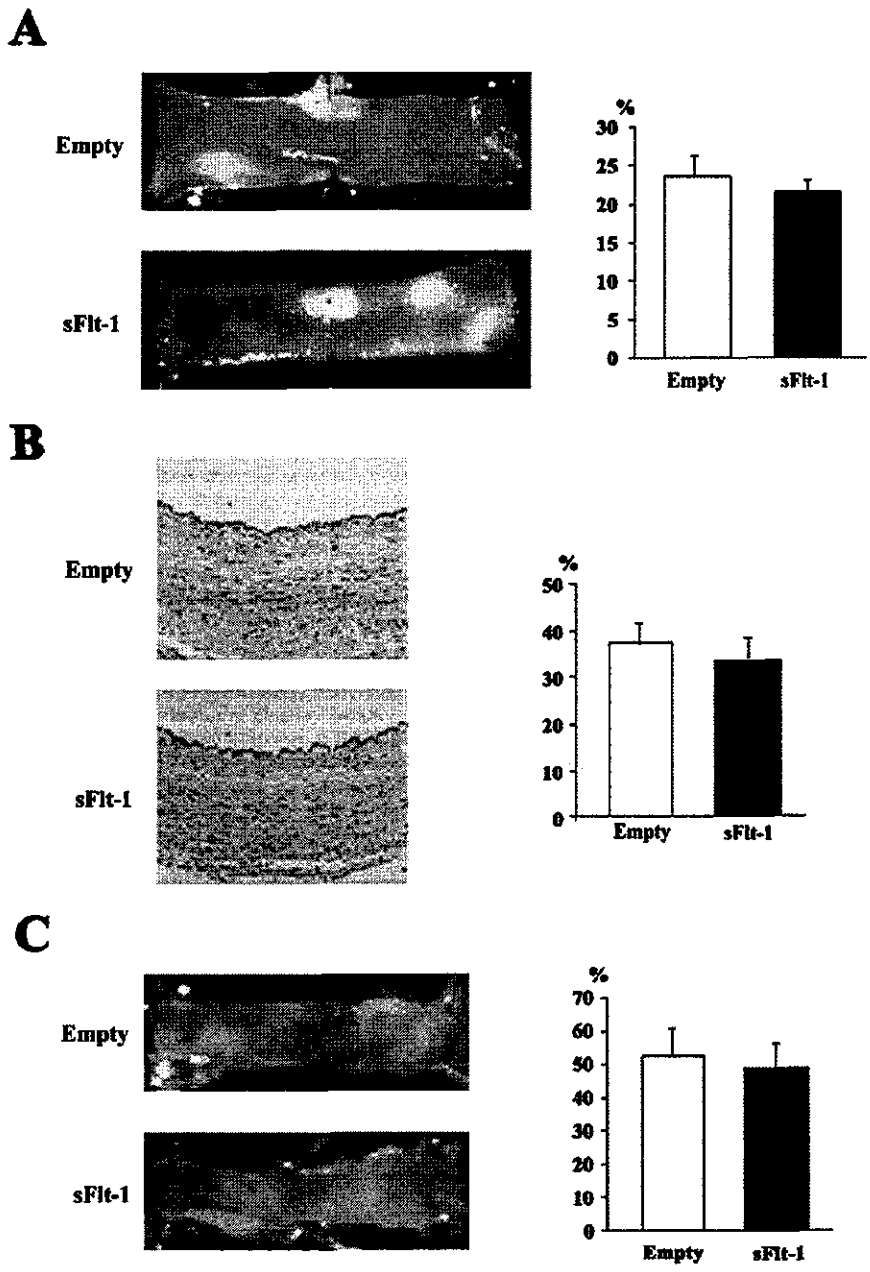

Figure 4. No significant effect of *sFlt-1* gene transfer on endothelial regeneration. A, Reendothelialization of rabbit carotid artery determined by Evans blue staining (deendothelialized areas are stained with blue) 7 days after balloon injury in rabbits. Endothelial regeneration of injured arteries was identified by intravenous injection of Evans blue dye 30 minutes before harvesting of vessels from rabbits and mice. Ratios of surface area covered by endothelium to total area in empty-plasmid and *sFlt-1* groups (n=7 each) are shown. B, Cross sections of rabbit femoral arteries stained with CD31 antibody 7 days after injury. Degrees of endothelial recovery (length of CD31-positive layer, length of internal elastic lamina in cross sections) in both groups are also shown (n=7 each). C, Reendothelialization of mouse femoral arteries 14 days after injury as determined by Evans blue staining (n=9 each).

and enhance neointimal formation after injury. In contrast to the conventional assumption, we here demonstrated that blockade of VEGF by *sFlt-1* gene transfer attenuated neointimal formation in rabbits, rats, and mice, indicating the essential role of VEGF in experimental restenosis.

As previously reported by others,[5–7,15] we demonstrated persistent increases in VEGF in arterial wall cells after injury. Emerging evidence suggests expression of functional VEGFR-1 and VEGFR-2 in cell types other than endothelial cells. We showed herein an increased expression of VEGFR-1 in lesional monocytes and medial smooth muscle cells during the early stage and in smooth muscle cells in the neointima and media during later stages. Increased VEGFR-2 expression was noted only at later stages. *sFlt-1* gene transfer attenuated the increased expression of inflammatory and growth factors such as VEGF, MCP-1, IL-1β, and so forth at early stages. Expression of VEGFR-1 in monocytes mediates chemotaxis,[9] and VEGFR-1 in smooth muscle cells mediates migration.[27] VEGFR-1 has been shown to act as an important mediator of VEGF-induced inflammation.[9,10,13] More recently, Yamada et al[28] showed that VEGF-mediated angiogenesis and inflammation are mediated by MCP-1. We also demonstrated the central role of MCP-1 in the mechanism of neointimal formation after vascular injury.[23–25,29] It is likely, therefore, that VEGF might cause vascular inflammation and migration of vascular smooth muscle cells and thus, cause neointimal formation after injury. Further studies are needed to elucidate the relative roles of VEGFR-1 and VEGFR-2 in the mechanisms of neointimal formation.

This study also demonstrated in rabbits the role of VEGF in the development of negative remodeling, another major cause of human restenosis after balloon angioplasty.[30] Fibro-

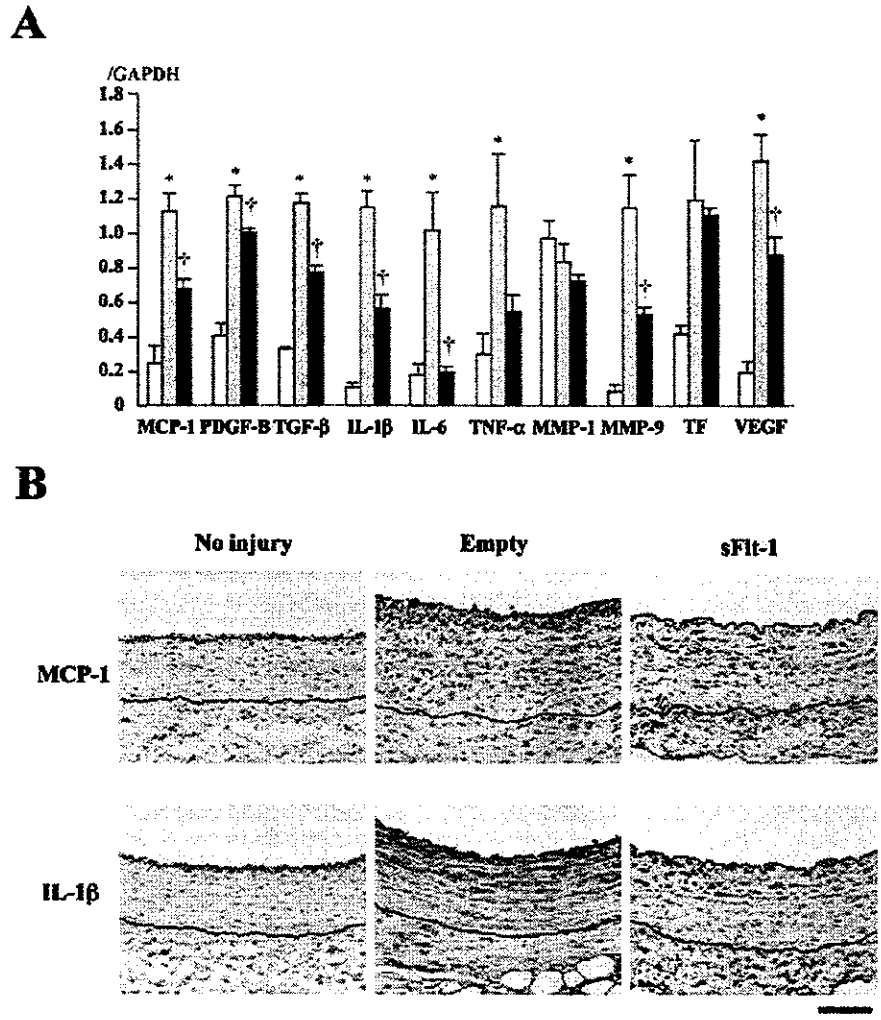

Figure 5. Inhibitory effect of *sFlt-1* gene transfer on expression of various inflammatory factors in rabbits. A, Effect of *sFlt-1* gene transfer on mRNA levels of various proinflammatory factors 1 day after injury. Quantitative real-time PCR was performed. *$P<0.01$ vs uninjured control (uninjured) artery; †$P<0.05$, ††$P<0.01$ vs empty-plasmid group. B, Carotid artery sections from control uninjured animals and those from empty-plasmid and *sFlt-1* groups 7 days after balloon injury stained immunohistochemically with MCP-1 and IL-1β. Internal and external elastic layers are highlighted with blue and black lines, respectively. Bar=100 μm. Immunohistochemical experiments were repeated 5 times, all with representative results.

sis and vasa vasorum in the adventitia have been implicated to be the central pathological processes leading to constrictive negative remodeling after balloon injury. Therefore, our present data suggest that *sFlt-1* gene transfer inhibited the development of negative constrictive remodeling by limiting adventitial fibrosis and angiogenesis.

VEGFR-1 has been shown to be an important mediator of stem cell recruitment and differentiation.[13] Sata and colleagues[26] have shown that a considerable proportion of neointimal and medial cells were bone marrow–derived progenitor cells. However, the role of VEGF in the recruitment and differentiation of progenitor cells into neointimal cells after vascular injury has not been addressed. We showed here that *sFlt-1* gene transfer inhibited recruitment of bone marrow–lineage cells into the peripheral circulation and injured arterial wall and thus, reduced neointimal formation after injury. These data suggest that VEGF might contribute to neointimal formation by recruiting bone marrow–derived and circulating monocytes.

Surprisingly, *sFlt-1* gene transfer did not affect endothelial regeneration after endothelial injury, suggesting a minor role of endogenous VEGF in endothelial regeneration after endothelial injury. It remains to be determined whether inhibition of VEGFR-2–mediated activity of endothelial regeneration by *sFlt-1* gene transfer might have been overshadowed by other stimuli (eg, basic fibroblast growth factor, angiopoietins, etc). On the contrary, adenovirus-mediated gene transfer of *VEGF* enhanced adventitial angiogenesis but did not reduce neointimal formation after balloon injury in rabbits. The latter observation is consistent with previous reports demonstrating that exogenous VEGF does not reduce neointimal formation in animals and humans.[15–17] Taken together, the role or mechanisms of action of VEGF may differ between exogenous and endogenous VEGF and between angiogenesis and neointimal formation.

This study may have significant clinical implications. First, *sFlt-1* gene transfer might be an attractive anti-VEGF therapy for inflammatory vascular disease and other inflammatory disorders. However, local delivery of *sFlt-1* must be preferable for clinical use to avoid potential side effects by systemic delivery. Second, our finding indicates that more research is required, especially on the safety of VEGF, before translational clinical research proceeds. Deleterious effects associated with overexpression of VEGF have recently been reported: (1) injection of VEGF-expressing skeletal muscle myoblasts into the murine heart caused the formation of hemangiomas and lethagenic heart failure[31] and (2) *VEGF* gene transfer into rabbit carotid arteries induced neointimal

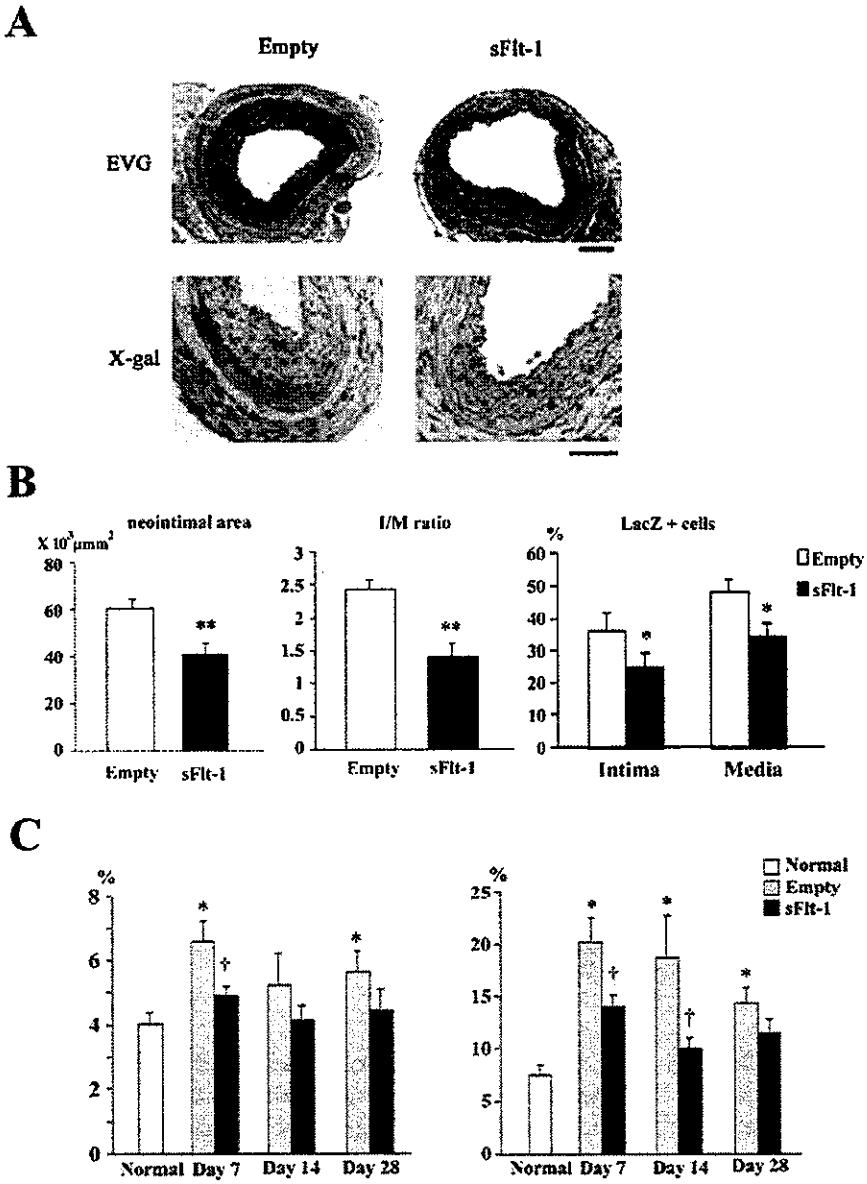

Figure 6. Contribution of bone marrow–derived cells to effect of *sFlt-1* gene transfer in mice. A, Arterial sections from empty-plasmid and *sFlt-1* groups 28 days after wire injury stained with X-gal or elastica van Gieson's (EVG) stains. Bar=100 μm. B, Inhibitory effects of *sFlt-1* gene transfer on neointimal formation (neointimal area and intima-media ratio) and percentage of LacZ-positive cells (100×LacZ-positive nuclei/total nuclei) in neointima and media. **P*<0.05, ***P*<0.01 vs phosphate-buffered saline, n=8 each. C, Summary of fluorescence-activated cell sorting analysis of recruitment of bone marrow–derived monocytes (left) and circulating monocytes (right) into peripheral circulation in normal mice and mice transfected with empty plasmid or *sFlt-1* after wire injury, n=7 or 8. **P*<0.05 vs normal mice (no injury); †*P*<0.05 vs empty-plasmid group.

formation with angiomatoid proliferation of endothelial cells.[12] These studies highlight the potential side effects or toxicity that would against the clinical use of VEGF for therapeutic angiogenesis and restenosis.

In conclusion, this study has provided direct in vivo evidence suggesting that increased expression and activity of VEGF are essential for the development of experimental restenosis after intraluminal injury by recruiting monocyte-lineage cells. Although there is no clinical evidence suggesting enhancement of atherosclerosis or neointimal formation by VEGF therapy,[16,17] our present data raise the question of whether VEGF therapy is useful without serious risks in patients with advanced atherosclerosis.

Acknowledgments

This study was supported by grants-in-aid for scientific research (14657172, 14207036) from the Ministry of Education, Science, and Culture, Tokyo, Japan; by health science research grants (Comprehensive Research on Aging and Health and Research on Translational Research) from the Ministry of Health Labor and Welfare, Tokyo, Japan; and by the Program for Promotion of Fundamental Studies in Health Sciences of the Organization for Pharmaceutical Safety and Research, Tokyo, Japan.

References

1. Folkman J. Angiogenesis in cancer, vascular, rheumatoid and other disease. *Nat Med.* 1995;1:27–31.
2. Carmeliet P, Jain RK. Angiogenesis in cancer and other diseases. *Nature.* 2000;407:249–257.
3. Ferrara N, Alitalo K. Clinical applications of angiogenic growth factors and their inhibitors. *Nat Med.* 1999;5:1359–1364.
4. Baumgartner I, Isner JM. Somatic gene therapy in the cardiovascular system. *Annu Rev Physiol.* 2001;63:427–450.
5. Inoue M, Itoh H, Ueda M, et al. Vascular endothelial growth factor (VEGF) expression in human coronary atherosclerotic lesions: possible pathophysiological significance of VEGF in progression of atherosclerosis. *Circulation.* 1998;98:2108–2116.
6. Chen YX, Nakashima Y, Tanaka K, et al. Immunohistochemical expression of vascular endothelial growth factor/vascular permeability factor in atherosclerotic intimas of human coronary arteries. *Arterioscler Thromb Vasc Biol.* 1999;19:131–139.
7. Shibata M, Suzuki H, Nakatani M, et al. The involvement of vascular endothelial growth factor and flt-1 in the process of neointimal prolif-

eration in pig coronary arteries following stent implantation. *Histochem Cell Biol.* 2001;116:471–481.
8. Isner JM. Still more debate over VEGF. *Nat Med.* 2001;7:639–640.
9. Barleon B, Sozzani S, Zhou D, et al. Migration of human monocytes in response to vascular endothelial growth factor (VEGF) is mediated via the VEGF receptor flt-1. *Blood.* 1996;87:3336–3343.
10. Kim I, Moon SO, Hoon Kim S, et al. Vascular endothelial growth factor expression of intercellular adhesion molecule-1 (ICAM-1), vascular cell adhesion molecule-1 (VCAM-1), and E-selectin through nuclear factor-κB activation in endothelial cells. *J Biol Chem.* 2001;276: 7614–7620.
11. Marumo T, Schini-Kerth VB, Busse R. Vascular endothelial growth factor activates nuclear factor-κB and induces monocyte chemoattractant protein-1 in bovine retinal endothelial cells. *Diabetes.* 1999;48: 1131–1137.
12. Yonemitsu Y, Kaneda Y, Morishita R, et al. Characterization of in vivo gene transfer into the arterial wall mediated by the Sendai virus (hemagglutinating virus of Japan) liposomes: an effective tool for the in vivo study of arterial diseases. *Lab Invest.* 1996;75:313–323.
13. Luttun A, Tjwa M, Moons L, et al. Revascularization of ischemic tissues by PlGF treatment, and inhibition of tumor angiogenesis, arthritis and atherosclerosis by anti-Flt1. *Nat Med.* 2002;8:831–40.
14. Celletti FL, Waugh JM, Amabile PG, et al. Vascular endothelial growth factor enhances atherosclerotic plaque progression. *Nat Med.* 2001;7: 425–429.
15. Hiltunen MO, Laitinen M, Turunen MP, et al. Intravascular adenovirus-mediated VEGF-C gene transfer reduces neointima formation in balloon-denuded rabbit aorta. *Circulation.* 2000;102:2262–2268.
16. Hedman M, Hartikainen J, Syvanne M, et al. Safety and feasibility of catheter-based local intracoronary vascular endothelial growth factor gene transfer in the prevention of postangioplasty and in-stent restenosis and in the treatment of chronic myocardial ischemia: phase II results of the Kuopio Angiogenesis Trial (KAT). *Circulation.* 2003;107: 2677–2683.
17. Henry TD, Annex BH, McKendall GR, et al. The VIVA trial: Vascular endothelial growth factor in Ischemia for Vascular Angiogenesis. *Circulation.* 2003;107:1359–1365.
18. Kendall RL, Wang G, Thomas KA. Identification of a natural soluble form of the vascular endothelial growth factor receptor, FLT-1, and its heterodimerization with KDR. *Biochem Biophys Res Commun.* 1996;226: 324–328.
19. Zhao Q, Egashira K, Inoue S, et al. Vascular endothelial growth factor is necessary in the development of arteriosclerosis by recruiting/activating monocytes in a rat model of long-term inhibition of nitric oxide synthesis. *Circulation.* 2002;105:1110–1115.
20. Goldman CK, Kendall RL, Cabrera G, et al. Paracrine expression of a native soluble vascular endothelial growth factor receptor inhibits tumor growth, metastasis, and mortality rate. *Proc Natl Acad Sci U S A.* 1998; 95:8795–8800.
21. Losordo DW, Vale PR, Hendel RC, et al. Phase 1/2 placebo-controlled, double-blind, dose-escalating trial of myocardial vascular endothelial growth factor 2 gene transfer by catheter delivery in patients with chronic myocardial ischemia. *Circulation.* 2002;105:2012–2018.
22. Kondo K, Hiratsuka S, Subbalakshmi E, et al. Genomic organization of the flt-1 gene encoding for vascular endothelial growth factor (VEGF) receptor-1 suggests an intimate evolutionary relationship between the 7-Ig and the 5-Ig tyrosine kinase receptors. *Gene.* 1998;208:297–305.
23. Usui M, Egashira K, Ohtani K, et al. Anti-monocyte chemoattractant protein-1 gene therapy inhibits restenotic changes (neointimal hyperplasia) after balloon injury in rats and monkeys. *FASEB J.* 2002;16: 1838–1840.
24. Mori E, Komori K, Yamaoka T, et al. Essential role of monocyte chemoattractant protein-1 in development of restenotic changes (neointimal hyperplasia and constrictive remodeling) after balloon angioplasty in hypercholesterolemic rabbits. *Circulation.* 2002;105:2905–2910.
25. Egashira K, Zhao Q, Kataoka C, et al. Importance of monocyte chemoattractant protein-1 pathway in neointimal hyperplasia after periarterial injury in mice and monkeys. *Circ Res.* 2002;90:1167–1172.
26. Sata M, Saiura A, Kunisato A, et al. Hematopoietic stem cells differentiate into vascular cells that participate in the pathogenesis of atherosclerosis. *Nat Med.* 2002;8:403–409.
27. Wang H, Keiser JA. Vascular endothelial growth factor upregulates the expression of matrix metalloproteinases in vascular smooth muscle cells: role of flt-1. *Circ Res.* 1998;83:832–840.
28. Yamada M, Kim S, Egashira K, et al. Molecular mechanism and role of endothelial monocyte chemoattractant protein-1 induction by vascular endothelial growth factor. *Arterioscler Thromb Vasc Biol.* 2003;23: 1996–2001.
29. Egashira K. Molecular mechanisms mediating inflammation in vascular disease: special reference to monocyte chemoattractant protein-1. *Hypertension.* 2003;41:834–841.
30. Kakuta T, Currier JW, Haudenschild CC, et al. Differences in compensatory vessel enlargement, not intimal formation, account for restenosis after angioplasty in the hypercholesterolemic rabbit model. *Circulation.* 1994;89:2809–2815.
31. Lee RJ, Springer ML, Blanco-Bose WE, et al. VEGF gene delivery to myocardium: deleterious effects of unregulated expression. *Circulation.* 2000;102:898–901.

Preclinica™
A Forum for Drug Development

Volume 2, No. 5 September/October, 2004

Novel Histoculture Drug Response Assay with a Simulated Microgravity Culture System

Katsuya Nakamura, Chihiro Nakahara, Hirotaka Kuga, Naoki Yamanaka, Akira Tasaki, Hiroshi Nakashima, Makoto Kubo, Takashi Morisaki, Hiroshi Fujii, Katsuo Sueishi, Masao Tanaka, and Mitsuo Katano
Kyushu University, Fukuoka, Japan

This study focused on the development of a next generation histoculture drug response assay (HDRA) that can provide information on chemosensitivity of carcinoma cells but not contaminating cells. For HDRA, we used a rotary cell culture system with four disposable vessels that provides a simulated microgravity (SM) condition. This new HDRA was named tentatively SM-HDRA. In SM-HDRA, we examined two types of carcinoma specimens, first, pancreatic carcinoma specimens transplanted into nude mice, and next, human carcinoma specimens resected surgically from 12 patients with colorectal or gastric carcinoma. The in vivo response of pancreatic carcinoma transplanted into nude mice was cultured in medium containing gemcitabine for 4 days. Human carcinoma specimens exposed to 5-fluorouracil (5-FU) or cisplatin (CDDP) were examined. The response was evaluated by hematoxylin-eosin staining, Ki-67 immunohistostaining, TUNEL assay, and secretion of carcinoembryonic antigen (CEA) and carbohydrate antigen 19-9 (CA19-9) into culture supernatants. Eleven of the twelve (91.6%) surgical specimens were successfully evaluated for SM-HDRA. SM-HDRA provided information not only about the chemosensitivity of carcinoma cells without interference from normal cells but also about heterogeneous drug responses in the carcinoma tissue, revealing different chemosensitivities. SM-HDRA is a new drug response assay and will be a useful tool for in-depth analyses of complicated carcinoma tissues and development of therapeutic strategies.

Reprinted with permission from Preclinica 2(5): 356-361 (September/October 2004)

INTRODUCTION

To individualize chemotherapies for cancer patients, in vitro drug response assays have been developed over the last five decades (1,2). Carcinoma tissues are complex systems comprising carcinoma cells, stromal cells, and extracellular matrix (3). In drug response assays, much attention has been given to development of an in vivo-like carcinoma model. Because many studies have indicated that the fiber distribution and biophysical architecture of collagen lattices closely resemble those of interstitial soft tissues, dermis, and network-like stroma of the lymph node (4), three-dimensional (3-D) hydrated collagen lattices have been widely used for in vivo-like culture of various types of carcinoma cells (5). In addition, several investigators have suggested that drug response may be a function of tissue architecture (6). In fact, 3-D cellular growth is an important factor affecting the chemosensitivities of carcinoma cells (7). On the basis of these findings, it is generally accepted that 3-D cultures are more useful than conventional 2-D cultures for evaluating chemosensitivities of carcinoma cells (6). Although 3-D cultures may be superior to 2-D cultures for drug response assays, differences between in vitro and in vivo drug responses indicate that factors, including barriers to drug penetration and microenvironmental conditions, other than the inherent chemosensitivity of the carcinoma cells influence the outcome of chemotherapy in vivo (8).

Table 1. Patient *Profiles* and Chemosensitivities

					Culture *Supernatants*[b]			
			SM-HDRA[a]		5-FU		CDDP	
Pt. No.	Origin	Age/Sex	5-FU	CDDP	CEA	CA19-9	CEA	CA19-9
1	rectum	76/M	49% (++)[c]	66% (+)	46%	65%	56%	48%
2	colon	67/M	48% (++)	93% (-)	49%	84%	75%	84%
3	stomach	22/F	100% (-)	95% (-)	109%	110%	111%	120%
4	colon	64/F	58% (+)	82% (-)	24%	112%	51%	116%
5	stomach	78/M	70% (+)	80% (-)	104%	34%	102%	40%
6	rectum	49/M	63% (+)	75% (-)	107%	11%	101%	51%
7	colon	68/M	68% (+)	87% (-)	40%	53%	70%	66%
8	stomach	39/M	61% (+)	75% (-)	49%	41%	72%	70%
9	rectum	43/M	71% (-)	81% (-)	60%	47%	72%	74%
10	stomach	81/M	9% (++)	62% (+)	N.D.	N.D.	N.D.	N.D.
11	stomach	71/M	61% (+)	75% (-)	N.D.	N.D.	N.D.	N.D.
12	stomach	52/M	—[d]	—	N.D.	N.D.	N.D.	N.D.

Pt. No., patient number; 5-FU, 5-fluorouracil; CDDP, cisplatin; CEA, carcinoembryonic antigen; CA19-9, carbohydrate antigen 19-9; N.D., not determined.

[a][(mean carcinoma cells/field with drug)/(mean carcinoma cells/field without drug)] × 100.

[b][(concentration in supernatant with drug)/(concentration in supernatant without drug)] × 100.

[c](++), ≤50% carcinoma cells, positive response; (+), 50%–70% carcinoma cells, weak response; (-), ≥70% carcinoma cells, negative response.

[d]very few carcinoma cells.

In 1951, Leighton (1) developed tissue cultures more similar to the in vivo situation by introducing a 3-D *sponge* matrix system. This approach was then termed histoculture by Sherwin et al. (9). Hoffman and colleagues (10–12) modified this tissue culture system into what they termed the histoculture drug response assay (HDRA). HDRA has been used successfully in a very high percentage of cases, and there is a strong correlation between drug response and survival of patients with various types of carcinoma, including gastric carcinoma (13), colon carcinoma (14), breast carcinoma (15), and head and neck carcinomas (16). HDRA is a technically simple and rapid assay (17). Because HDRA is usually evaluated with the 3-(4,5-dimetylthiazol-2-yl)-2,5-diphenyl-2H tetrazolium bromide (MTT) end point (18) or ^{3}H-thymidine (^{3}H-TdR) incorporation end point (12), it is difficult to exclude the influence of the drug responses of co-existing normal cells. It is also difficult to determine if the heterogeneous carcinoma cells that make up a carcinoma tissue have variable responses to the drugs. Thus, it is difficult to select a suitable chemotherapeutic agent or combination of chemotherapeutic drugs to effectively kill all carcinoma cells on the basis of HDRA data alone.

A novel 3-D culture system that creates a simulated microgravity (SM) (about 10^{-2} g) environment on earth was developed at the NASA Johnson Space Center (19). Recent studies have suggested that microgravity influences cellular functions such as proliferation (20,21), signal transduction (22,23), and gene expression (24–26). We have previously reported that both a 3-D carcinoma tissue model and pancreatic carcinoma specimens cultured under SM conditions with a RCCS™-4DQ system maintained both the histopathological and biological characteristics of the original carcinoma tissue (27). Advantages of the SM culture system have also been reported by other investigators (28–33). It has been indicated that SM conditions may provide controlled supplies of oxygen and nutrients with minimal turbulence and extremely low shear stress (34). In the present study, we attempted to develop a novel HDRA that incorporates the SM culture system. This new HDRA was tentatively named SM-HDRA. We also describe how SM-HDRA might make it possible to overcome the heterogeneous drug responses of complex carcinoma tissues.

RESULTS

We examined the carcinoma specimens resected from nude mice transplanted with NOR-P1 cells. NOR-P1 cells were injected subcutaneously into nude mice, and NOR-P1 carcinoma masses were resected surgically as described in the Materials and Methods. These tissues were cultured with the indicated concentrations (0.1–10 μM) of gemcitabine for 4 days under SM conditions. Carcinoma tissues isolated from nude mice closely resembled both histopathologically and biologically the original carcinoma tissue (Figure 1A). The numbers of carcinoma cells and Ki-

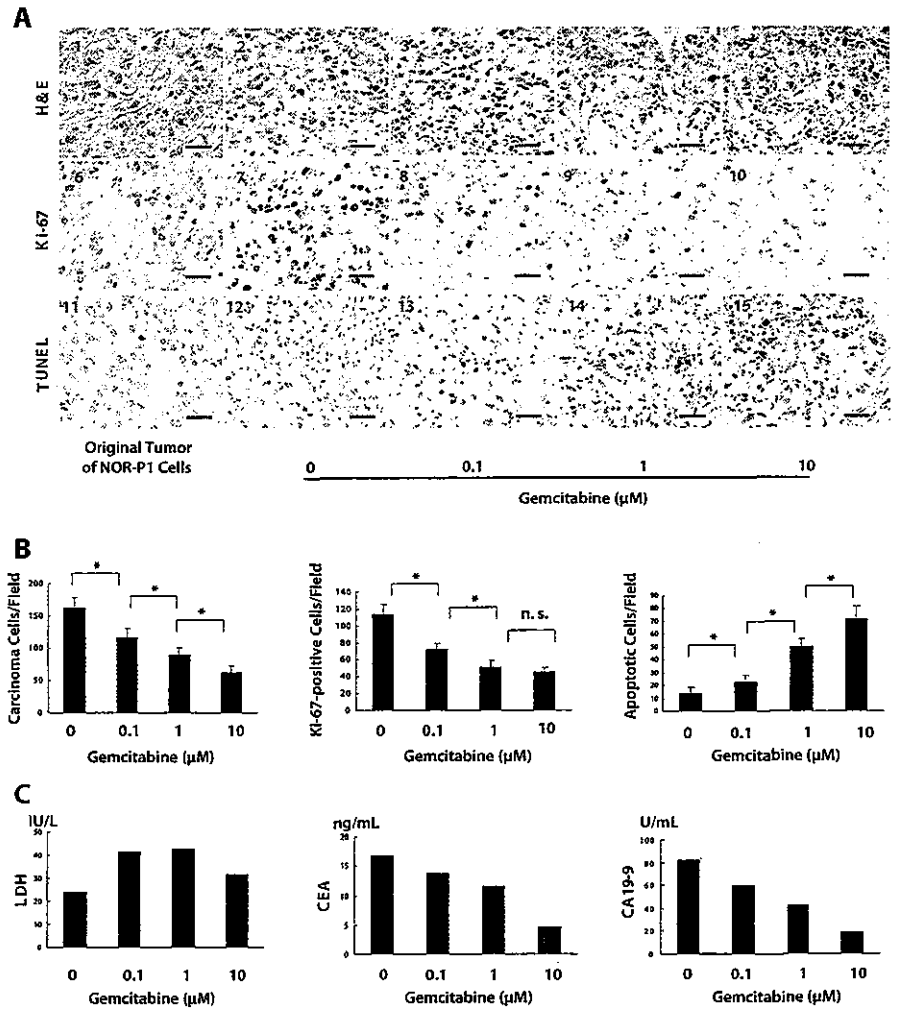

Figure 1. SM-HDRA with NOR-P1 tumors growing in nude mice. (A) Carcinoma cells (panels 1–5), cycling cells (panels 6–10), and apoptotic cells (panels 11–15) were determined by use of hematoxylin and eosin (H&E) staining, anti-Ki-67 antibody, and the TUNEL method, respectively. Original tumor of NOR-P1 cells (panels 1,6,11). (B) Quantitation of carcinoma cells/field, Ki-67-positive cells/field, and apoptotic cells/field. (C) Concentrations of lactate dehydrogenase (LDH), carcinoembryonic antigen (CEA), and carbohydrate antigen 19-9 (CA19-9) in culture supernatants. Bars, 50 μm. Mean ± SD of triplicate experiments. *, $P < 0.01$. SM-HDRA, histoculture drug response assay under simulated microgravity condition.

67-positive cells decreased and that of apoptotic cells increased as the dose of gemcitabine was increased (Figure 1, A and B). The effective dose was ≥1 μM of gemcitabine. Concentrations of both carcinoembryonic antigen (CEA) and carbohydrate antigen 19-9 (CA19-9) in culture supernatants decreased, and lactate dehydrogenase (LDH) concentration increased as the dose of gemcitabine increased (Figure 1C).

NOR-P1 carcinoma-bearing nude mice received intraperitoneal injections of gemcitabine (250 mg/kg) as described in the Materials and Methods. Gemcitabine significantly suppressed the growth of established NOR-P1 carcinomas (Figure 2A). Histopathological (Figure 2B) and biological findings (Figure 2C, in vivo response) were similar to those of SM-HDRA (in vitro response) at 10 μM gemcitabine (Figure 1).

Carcinoma specimens were resected surgically from 12 patients with carcinoma (six gastric and six colorectal carcinomas). Eleven of the 12 carcinoma specimens were evaluated successfully with SM-HDRA. One specimen that contained only a small number of carcinoma cells was judged to be an unsuitable case. Results are summarized in Table 1.

Patient 1 (Pt. No. 1 in Table 1) was a 76-year-old man with advanced rectal carcinoma. In this case, the 5-fluorouracil (5-FU) response was positive, and the cisplatin (CDDP) response was weak (Table 1). The specimen secreted a large amount of CEA (500 ng/mL) and a small amount of CA19-9 (30 U/mL). After surgery, serum CEA concentrations (normal level <2.5 ng/mL) decreased from 10.2 to 2.3 ng/mL. Serum level of CA19-9 (normal level <37 U/mL) was <23 U/mL. He received 500 mg uracil-tegafur (UFT) as tegafur three times daily perorally. No signs of recurrence, including changes in serum CEA and CA19-9 levels have been identified at the time of this writing (6 postoperative months).

Patient 2 (Pt. No. 2 in Table 1) was a 67-year-old man with advanced colon carcinoma. In this case, the 5-FU response was positive, and the CDDP response was negative (Table 1). The specimen secreted both CEA (200 ng/mL) and CA19-9 (250 U/mL). After surgery, his serum CEA concentration decreased from 2.9 to 1.2 ng/mL. The patient is presently receiving 500 mg UFT as tegafur three times daily perorally. No signs of recurrence have been noted as of this writing (6 postoperative months).

Patient 3 (Pt. No. 3 in Table 1) was a 22-year-old woman with advanced gastric carcinoma. In this case, both 5-FU and CDDP responses were negative (Table 1). The specimen secreted small amounts of CEA (28 ng/mL) and CA19-9 (33 U/mL). The patients received no chemotherapeutic drugs after surgery. After surgery, her serum CA19-9 level increased rapidly from 56 to 1622 U/mL. Her CEA level was <2.5 ng/mL.

In patient 2, the 5-FU response was positive in SM-HDRA (Table 1). It appears that 5-FU suppressed CEA secretion from the carcinoma specimen. However, 5-FU did not suppress CA19-9 secretion (Table 1). The response to CDDP was negative and had no effect on CEA or CA19-9 secretion. These findings suggest that 5-FU is effective against CEA-producing carcinoma cells but is ineffective against CA19-9-producing carcinoma cells. Specimens were stained with anti-CEA or anti-CA19-9 antibodies (Figure 3A). As we expected, the number of CEA-producing carcinoma cells, but not CA19-9-producing carcinoma cells, was decreased in response to 5-FU.

In patient 3, response to both 5-FU and CDDP was negative in SM-HDRA and had no effect on CEA or CA19-9 secretion (Table 1). The number of CEA-producing cells and the intensity of CEA staining were not affected significantly by 5-FU or CDDP (Figure 3B). Similarly, neither 5-FU nor CDDP influenced the number of CA19-9-positive carcinoma cells or intensity of CA19-9 staining.

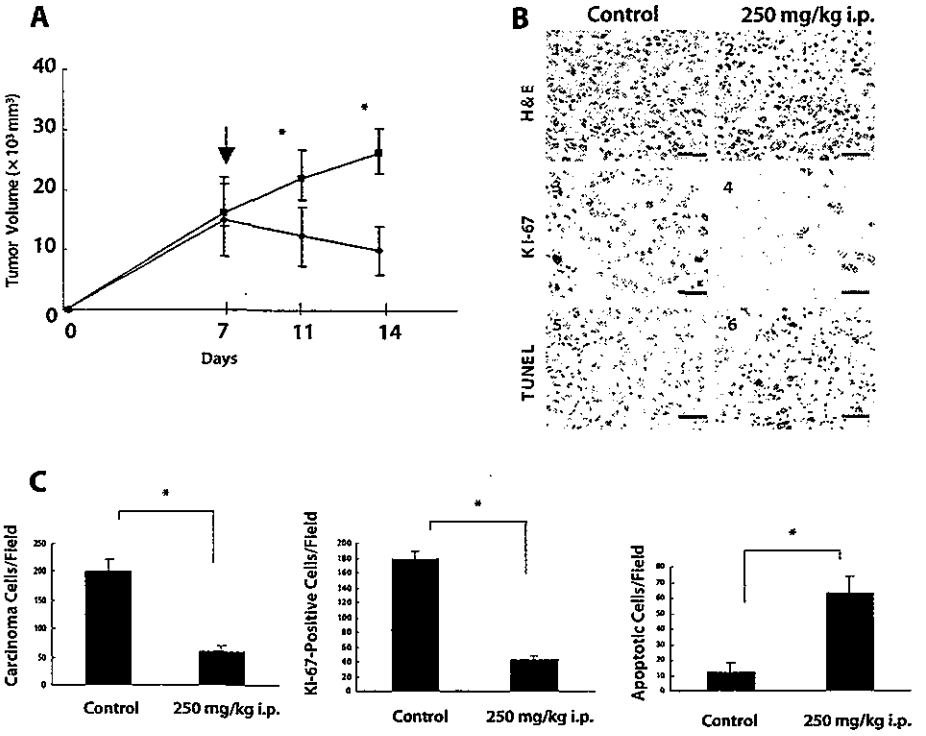

Figure 2. Effect of gemcitabine on NOR-P1 cells growing as tumors in nude mice. (A) Intraperitoneal (i.p.) administration of gemcitabine (250 mg/kg) on day 7 (arrow). (—■—, control; —●—, gemcitabine). (B) Carcinoma cells (panels 1 and 2), cycling cells (panels 3 and 4), and apoptotic cells (panels 5 and 6) were determined by use of hematoxylin and eosin (H&E) staining, anti-Ki-67 antibody, and the TUNEL method, respectively. (C) Quantitation of carcinoma cells/field, Ki-67-positive cells/field, and apoptotic cells/field. Bars, 50 μm. Mean ± SD of triplicate experiments. *, $P < 0.05$.

DISCUSSION

We describe here the development of a novel HDRA methodology, SM-HDRA, that uses the SM culture system. SM-HDRA may be useful for evaluation of both the chemosensitivity of carcinoma cells without the interference of normal cells and the heterogeneous responses of individual carcinoma cells to various chemotherapeutic agents.

Because carcinoma tissue consists of a complex mix of various components, including carcinoma cells, stromal cells, and extracellular matrix, chemosensitivity and several additional factors, such as drug penetration or microenvironmental conditions, influence drug responses in vivo (8). In particular, the 3-D architecture of the carcinoma tissue is an important factor in the drug response of each cancer patient (6). Leighton (1) developed a tissue culture system that mimics the in vivo situation with a 3-D sponge matrix. This system has been improved by several investigators (9,35) and applied to HDRA for individualizing chemotherapies to many kinds of carcinomas (10–12). Several studies have shown that HDRA is correlated with in vivo sensitivity and resistance of carcinoma cells and survival prognosis for the patient (12–16,36). Because HDRA is evaluated from the MTT (18) or ^{3}H-TdR-incorporation end points (12), it can not exclude the responses of normal cells such as fibroblasts or lymphocytes to chemotherapeutic agents, especially cytotoxic agents. In addition, carcinomas are complex systems consisting of heterogeneous carcinoma cells that show different chemosensitivities to each drug (10). It is difficult to evaluate heterogeneous drug responses in carcinoma tissues by conventional drug response assays including HDRA. To address these problems, we combined SM culture and histoculture systems. We previously reported that the SM culture system maintains both the architecture of the carcinoma tissue and the biological characteristics of the carcinoma cells in the original carcinoma tissue and that this allowed discrimination of carcinoma cells from other cells microscopically (27). With SM-HDRA, we could evaluate with considerable precision the chemosensitivities of carcinoma cells without interference from normal cells (Figures 1 and 2). Our preliminary study indicated that carcinoma cells secrete larger amounts of CEA and CA19-9 under SM culture conditions in comparison with 1 g culture conditions (unpublished data). In fact, there have been few reports concerning protein secretion by tissues under SM culture conditions (32). In SM-HDRA, all nine carcinoma specimens secreted measurable levels of CEA and CA19-9 into the culture medium (Table 1). Both CEA and CA19-9 are secreted by carcinoma cells but not normal cells present in the carcinoma tissue. The numbers of carcinoma cells counted in SM-

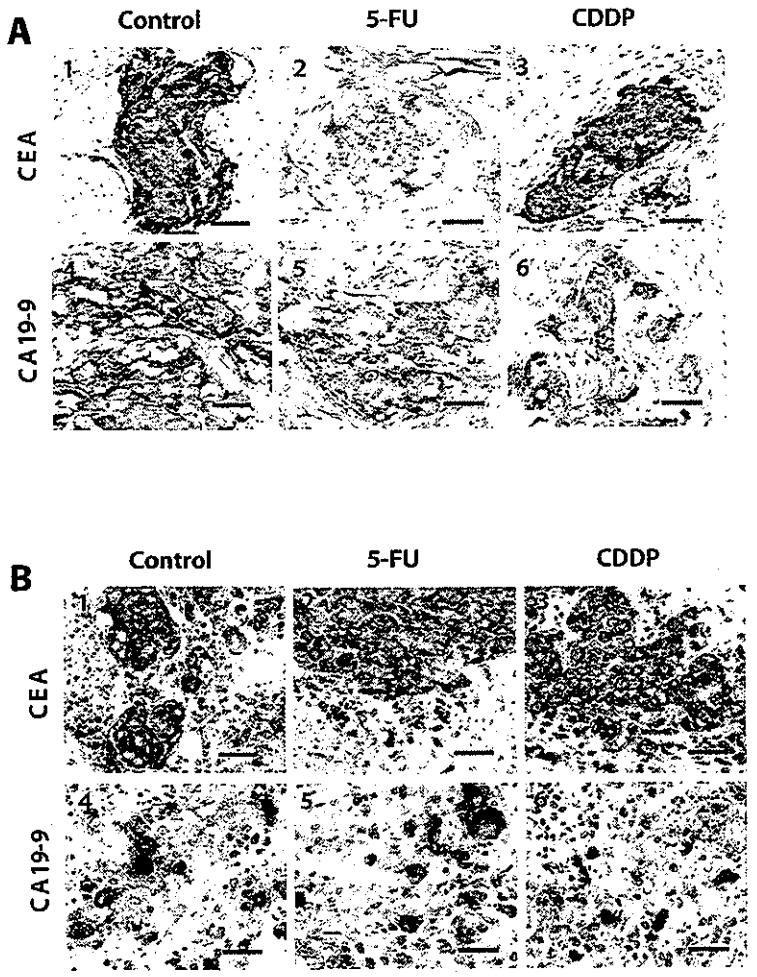

Figure 3. CEA and CA19-9 immunostaining of carcinoma specimens. (A) CEA-producing cells (panels 1–3) and CA19-9-producing cells (panels 4–6) in patient 2 were determined by use of anti-CEA antibody and anti-CA19-9 antibody, respectively. (B) CEA-producing cells (panels 1–3) and CA19-9-producing cells (panels 4–6) in patient 3 were determined by use of anti-CEA antibody and anti-CA19-9 antibody, respectively. Bars, 50 μm. CEA, carcinoembryonic antigen; CA19-9, carbohydrate antigen 19-9; 5-FU, 5-fluorouracil; CDDP, cisplatin.

HDRA were well correlated with CEA and/or CA19-9 concentration (Figures 1 and 2). This finding strongly suggests that the cells counted in SM-HDRA are carcinoma cells and not normal cells. If so, we may be able to evaluate drug responses from CEA and CA19-9 concentrations in the culture medium. Measurements of both CEA and CA19-9 concentrations suggested that SM-HDRA may provide information about the heterogeneous drug responses of a carcinoma sample. For example, in patient 2, 5-FU decreased CEA secretion by carcinoma but did not affect CA19-9 secretion, suggesting that the carcinoma specimen may contain at least two types of carcinoma cells, CEA-producing carcinoma cells and CA19-9-producing carcinoma cells. This possibility is supported by our data showing that 5-FU markedly decreased the number of CEA-positive cells but had no effect on the number of CA19-9-positive cells (Pt. No. 2 in Table 1). From these results, we speculated that 5-FU is effective against CEA-positive cells but not CA19-9-positive cells in patient 2. If this hypothesis is correct, the patient should be treated with a drug effective against CA19-9-positive carcinoma cells. In patient 3, only CA19-9 increased rapidly 2 months after surgery. The carcinoma tissue obtained during surgery contained both CEA- and CA19-9-positive cells. We now suspect that the CA19-9-producing carcinoma cells grow more rapidly than the CEA-producing carcinoma cells in this case.

The present study suggests that SM-HDRA may be not only a new drug response assay but also a powerful tool for development of therapeutic strategies. Using SM-HDRA, we may be able to evaluate the differential chemosensitivities of carcinoma cells in complex carcinoma tissue without interference from normal cells. However, further clinical studies are needed before SM-HDRA is viable for routine clinical use.

MATERIALS AND METHODS

NOR-P1 Carcinoma in Nude Mice

Six-week-old female athymic nude mice (BALBc nu/nu) were purchased from Japan SLC (Hamamatsu, Japan). The mice were housed in laminar flow cabinets under specific pathogen-free condition in facilities approved by Kyushu University. All surgical procedures were done under general anesthesia with ether. Human pancreatic carcinoma cells, NOR-P1, were grown in RPMI 1640 (Gibco BRL, Grand Island, NY) containing 10% fetal calf serum (FCS; Gibco BRL) (37). NOR-P1 cells (5×10^6 cells/0.2 mL) were transplanted subcutaneously into nude mice (37). One week after transplantation, each tumor mass (approximately 1 cm in diameter) was resected surgically.

Effect of Gemcitabine on the Growth of NOR-P1 Cells Transplanted into Nude Mice

HCL, 2′,2′-difluorodeoxycytidine (gemcitabine) was purchased from Eli Lilly (Indianapolis, IN). NOR-P1 cells (5×10^6 cells/0.2 mL) were implanted subcutaneously into 6-week-old female BALBc nude mice on day 0, and tumor diameters were measured with a Vernier caliper. Tumor volume (TV) was calculated according to the following formula: $TV\ (mm^3) = d^2 \times D/2$, where d and D are the shortest diameter and longest diameter, respectively. On day 7, 250 mg/kg of gemcitabine was injected intraperitoneally. On day 14, the tumor mass was resected surgically and examined histopathologically.

HDRA Under SM Condition

Carcinoma specimens were obtained during surgery from 12 patients with gastric or colorectal carcinoma. We never failed to take informed consent from each patient before those preparations. Each carcinoma specimen was rinsed three times with phosphate-

buffered saline (PBS) and minced with a sterile scalpel into pieces of approximately 1–2 mm^3. The pieces were rinsed again with RPMI 1640 medium to eliminate single or aggregated cells. Pieces of approximately 2 mm^3 were selected for SM-HDRA. For histoculture under SM condition, we used a NASA bioreactor, which is a rotary cell culture system with four disposable vessels (RCCS-4DQ; Synthecon, Houston, TX). A 3-D pancreatic carcinoma model (2 mm^3) or a 2-mm^3 piece of carcinoma tissue was placed into a 10-mL volume disposable vessel. The vessel was then filled completely with RPMI 1640 containing 10% FCS with or without chemotherapeutic agent. 5-FU was purchased from Kyowa Hakko Kogyo Ltd. (Tokyo, Japan). CDDP was purchased from Bristol-Myers Squibb K.K. (Tokyo, Japan). The concentrations of chemotherapeutic agents used in this study were 0.1–10 μM for gemcitabine (38), 300 μg/mL for 5-FU (36), and 20 μg/mL for CDDP (36). The bioreactor was then rotated on a rotary cell culture system power supply (Model PS-4; Synthecon) at an initial speed of 20 rpm. The rotation speed was adjusted so that tumor pieces remained in a state of free fall as described previously (27).

After 4 days of initial SM culture, a small piece of carcinoma was removed from each vessel, fixed with buffered formalin (10% methanol, 4% formaldehyde), and embedded in paraffin for histochemical or immunohistochemical analysis. Paraffin-embedded sections were stained with hematoxylin and eosin (H&E). Response of carcinoma cells to each chemotherapeutic agent was evaluated by counting carcinoma cells without nuclear fragmentation. Carcinoma cells were pathologically identified under microscope. We counted the number of carcinoma cells in 10 random fields/section at magnification of ×200. The mean number of carcinoma cells per 10 fields was expressed as carcinoma cells/field. When the carcinoma cell number was less than 50% in comparison with controls, the response of cells was considered positive. When the number of carcinoma cells was 50%–70% and >70%, the response was considered weak and negative, respectively.

Culture supernatants were also collected and filtrated with 0.20-μm pore filter (Minisart®; Sartorius, Edgewood, NY) from each vessel after 4 days of initial culture and stored at -20°C until use. Concentrations of lactate dehydrogenase (LDH), CEA, and CA19-9 in the supernatants were examined for nine specimens. Concentrations of LDH, CEA, and CA19-9 were determined by CicaLiquid LDH (Kanto Chemical, Tokyo, Japan), ARCHITECT™ i2000™ (Dinabot, Ciba, Japan), and CA19-9 RIA kit (Fuji Rebio Diagnostic, Tokyo, Japan), respectively. The detection limits for LDH, CEA, and CA19-9 were 5 IU/mL, 0.5 ng/mL, and 6 U/mL, respectively.

Immunohistochemical Analysis

Immunohistochemical staining of Ki-67, CEA, and CA19-9 were done with anti-Ki-67, anti-CEA, and anti-CA19-9 (all from DAKO A/S, Glostrup, Denmark), respectively, as described previously (27). Apoptotic cells were evaluated by in situ TUNEL labeling as described previously (27). Nuclei were counterstained with H&E. Ten fields were selected at random under high-power light microscopy. The mean numbers of Ki-67- and TUNEL-positive cells were expressed as the Ki-67-positive cells/field and apoptotic cells/field, respectively.

Statistical Analysis

All results are expressed as mean ± standard deviation (SD). The statistical significance of differences between group means was assessed with the Student's *t*-test. All results with a P value of <0.05 were considered statistically significant.

ACKNOWLEDGMENTS

This study was supported by Grant-in-Aid for General Scientific Research (Nos. 14571143 and 15390380) from the Ministry of Education, Culture, Sports, Science, and Technology of Japan. We thank T. Kanemaru and K. Nomiyama for excellent technical assistance.

COMPETING INTERESTS STATEMENT

The authors declare no conflicts of interest.

REFERENCES

1. **Leighton, J.** 1951. A sponge matrix method for tissue cultures. Formation of organized aggregates of cells in vitro. J. Natl. Cancer Inst. *50*:545-561.
2. **Kern, D.H., M.A. Campbell, A.J. Cochran, M.W. Burk, and D.L. Morton.** 1982. Cloning of human solid tumors in soft agar. Int. J. Cancer *30*:725-729.
3. **Matrisian, L.M., G.R. Cunha, and S. Mohla.** 2001. Epithelial-stromal interactions and tumor progression: meeting summary and future directions. Cancer Res. *61*:3844-3846.
4. **Elsdale, T. and J. Bard.** 1972. Collagen substrata for studies on cell behavior. J. Cell. Biol. *41*:298-311.
5. **Friedl, P., P.B. Noble, P.A. Walton, D.W. Laird, P.J. Chauvin, R.J. Tabah, et al.** 1995. Migration of coordinated cell clusters in mesenchymal and epithelial cancer explants in vitro. Cancer Res. *55*:4557-4560.
6. **Hoffman, R.M.** 1993. To do tissue culture in two or three dimensions? That is the question. Stem Cells *11*:105-111.
7. **Furukawa, T., T. Kubota, M. Watanabe, S. Kase, Y. Saikawa, H. Nishibori, et al.** 1992. Increased drug resistance of cultured human cancer cell lines in a three-dimensional cellular growth assay using collagen gel matrix. J. Surg. Oncol. *49*:86-92.
8. **Phillips, R.M., M.C. Bibby, and J.A. Double.** 1990. A critical appraisal of the predictive value of in vitro chemosensitivity assays. J. Natl. Cancer Inst. *82*:1457-1468.
9. **Sherwin, R.P., A. Richters, A.E. Yellin, and A.J. Donavan.** 1980. Histoculture of human breast cancers. Surg. Oncol. *13*:9-20.
10. **Hoffman, R.M.** 1991. In vitro sensitivity assays in cancer: a review, analysis, and prognosis. J. Clin. Lab. Anal. *5*:133-143.
11. **Hoffman, R.M.** 1993. In vitro assays for chemotherapy sensitivity. Crit. Rev. Oncol. Hematol. *15*:99-111.

12. **Vescio, R.A., K.M. Connors, G.M. Bordin, J.A. Robb, T. Youngkin, J.N. Umbreit, et al.** 1990. The distinction of small cell and non-small cell cancer by growth in native-state histoculture. Cancer Res. *50*:6095-6099.
13. **Kubota, T., T. Egawa, Y. Otani, T. Furukawa, Y. Saikawa, M. Yoshida M, et al.** 2003. Cancer chemotherapy chemosensitivity testing is useful in evaluating the appropriate adjuvant cancer chemotherapy for stage III/IV gastric cancers without peritoneal dissemination. Anticancer Res. *23*:583-587.
14. **Isshi, K., T. Sakuyama, T. Gen, Y. Nakamura, T. Kuroda, T. Katuyama, et al.** 2002. Predicting 5-FU sensitivity using human colorectal cancer specimens: comparison of tumor dihydropyrimidine dehydrogenase and orotate phosphoribosyl transferase activities with in vitro chemosensitivity to 5-FU. Int. J. Clin. Oncol. *7*:335-342.
15. **Tanino, H., S. Oura, R.M. Hoffman, T. Kubota, T. Furukawa, J. Arimoto, et al.** 2001. Acquisition of multidrug resistance in recurrent breast cancer demonstrated by the histoculture drug response assay. Anticancer Res. *21*:4083-4086.
16. **Singh, B., R. Li, L. Xu, A. Poluri, S. Patel, A.R. Shaha, et al.** 2002. Prediction of survival in patients with head and neck cancer using the histoculture drug response assay. Head Neck *24*:437-442.
17. **Furukawa, T., T. Kubota, M. Watanabe, T. Takahara, H. Yamaguchi, T. Takeuchi, et al.** 1992. High in vivo-in vitro correlation of drug response using sponge-gel-supported three-dimensional histoculture and the MTT end point. Int. J. Cancer *51*:489-498.
18. **Furukawa, T., T. Kubota, M. Watanabe, M. Kitajima, and R.M. Hoffman.** 1993. A novel "patient-like" treatment model of human pancreatic cancer constructed using orthotopic transplantation of histologically intact human tumor tissue in nude mice. Cancer Res. *53*:3070-3072.
19. **Lelkes, P.I., D.L. Galvan, G.T. Hayman, T.J. Goodwin, D.Y. Chatman, S. Cherian, et al.** 1998. Simulated microgravity conditions enhance differentiation of cultured PC12 cells towards the neuroendocrine phenotype. In Vitro Cell. Dev. Biol. Anim. *34*:316-325.
20. **Hughes-Fulford, M. and M.L. Lewis.** 1996. Effects of microgravity on osteoblast growth activation. Exp. Cell Res. *224*:103-109.
21. **Moos, P.J., H.K. Fattaey, and T.C. Johnson.** 1994. Cell proliferation inhibition in reduced gravity. Exp. Cell Res. *213*:458-462.
22. **Boonstra, J.** 1999. Growth factor-induced signal transduction in adherent mammalian cells is sensitive to gravity. FASEB J. *13(Suppl)*:S35-S42.
23. **Hatton, J.P., F. Gaubert, M.L. Lewis, Y. Darsel, P. Ohlmann, J.P. Cazenave, et al.** 1999. The kinetics of translocation and cellular quantity of protein kinase C in human leukocytes are modified during spaceflight. FASEB J. *13(Suppl)*: S23-S33.
24. **Carmeliet, G. and R. Bouillon.** 1999. The effect of microgravity on morphology and gene expression of osteoblasts *in vitro*. FASEB J. *13(Suppl)*:S129-S134.
25. **Nash, P.V. and A.M. Mastro.** 1992. Variable lymphocyte responses in rats after space flight. Exp. Cell Res. *202*:125-131.
26. **Walther, I., P. Pippia, M.A. Meloni, F. Turrini, F. Mannu, and A. Cogoli.** 1998. Simulated microgravity inhibits the genetic expression of interleukin-2 and its receptor in mitogen-activated T lymphocytes. FEBS Lett. *436*:115-118.
27. **Nakamura, K., H. Kuga, T. Morisaki, E. Baba, N. Sato, K. Mizumoto, et al.** 2002. Simulated microgravity culture system for a 3-D carcinoma tissue. BioTechniques *33*:1068-1076.
28. **Goodwin, T.J., W.F. Schroeder, D.A. Wolf, and M.P. Moyer.** 1993. Rotating-wall vessel coculture of small intestine as a prelude to tissue modeling: aspect of simulated microgravity. Proc. Soc. Exp. Biol. Med. *202*:181-192.
29. **Cogoli, A., B. Bechler, M. Cogoli-Greuter, S.B. Criswell, H. Joller, P. Loller, et al.** 1993. Mitogenic signal transduction in T lymphocytes in microgravity. J. Leukoc. Biol. *53*:569-575.
30. **Prewett, T.L., T.J. Goodwin, and G.F. Spaulding.** 1993. Three-dimensional modeling of T-24 human bladder carcinoma cell line: a new simulated microgravity culture vessel. J. Tiss. Cult. Methods *15*:29-36.
31. **Jessup, J.M., T.J. Goodwin, and G. Spaulding.** 1993. Prospects for use of microgravity-based bioreactors to study three-dimensional host-tumor interactions in human neoplasia. J. Cell Biochem. *51*:290-300.
32. **Rutzky, L.P., S. Bilinski, M. Kloc, T. Phan, H. Zhang, S.M. Katz, et al.** 2002. Microgravity culture condition reduces immunogenicity and improves function of pancreatic islets. Transplantation *74*:13-21.
33. **Licato, L.L., V.G. Prieto, and E.A. Grimm.** 2001. A novel preclinical model of human malignant melanoma utilizing bioreactor rotating-wall vessels. In Vitro Cell. Dev. Biol. Anim. *37*:121-126.
34. **Goodwin, T.J., T.L. Prewett, D.A. Wolf, and G.F. Spaulding.** 1993. Reduced shear stress: a major component in the ability of mammalian tissues to from three-dimensional assemblies in simulated microgravity. J. Cell Biochem. *51*:301-311.
35. **Yoshida, Y., V. Hilborn, and A.E. Freeman.** 1980. Fine structure identification of organoid mouse ling cells cultured on a pigskin substrate. In Vitro *16*:994-1006.
36. **Furukawa, T., T. Kubota, and R.M. Hoffman.** 1995. Clinical application of the histoculture drug response assay. Clin. Cancer Res. *1*:305-311.
37. **Sato, N., K. Mizumoto, K. Beppu, N. Maehara, M. Kusumoto, T. Nabae, et al.** 2000. Establishment of a new human pancreatic cancer cell line, NOR-P1, with high angiogenic activity and metastatic potential. Cancer Lett. *155*:153-161.
38. **Bruns, C.J., M.T. Harbison, D.W. Davis, C.A. Portera, R. Tsan, D.J. McConkey, et al.** 2000. Epidermal growth factor receptor blockade with C225 plus gemcitabine results in regression of human pancreatic carcinoma growing orthotopically in nude mice by antiangiogenic mechanisms. Clin. Cancer Res. *6*:1936-1948.

Address correspondence to:

Mitsuo Katano
Department of Cancer Therapy and Research
Graduate School of Medical Sciences
Kyushu University
3-1-1 Maidashi
Higashi-ku, Fukuoka 812-8582, Japan
e-mail: mkatano@tumor.med.kyushu-u.ac.jp

Available online at www.sciencedirect.com
SCIENCE DIRECT®
ELSEVIER
Pathology – Research and Practice 200 (2004) 517–529
PATHOLOGY
RESEARCH AND PRACTICE
www.elsevier.de/prp

ORIGINAL ARTICLE

Growth pattern correlates with the distribution of basement membrane and prognosis in lung adenocarcinoma

Yoshio Matsuo[a], Shuichi Hashimoto[a], Takaomi Koga[a], Yoshikazu Yonemitsu[a], Ichiro Yoshino[b], Keizo Sugimachi[b], Hiroshi Honda[c], Koji Masuda[c], Katsuo Sueishi[a,*]

[a] *Pathophysiological and Experimental Pathology, Department of Pathology, Graduate School of Medical Sciences, Kyushu University 60, 3-1-1, Higashi-ku, Fukuoka 812-8582, Japan*
[b] *General Surgery, Graduate School of Medical Sciences, Kyushu University 60, 3-1-1, Higashi-ku, Fukuoka 812-8582, Japan*
[c] *Clinical Radiology, Graduate School of Medical Sciences, Kyushu University 60, 3-1-1, Higashi-ku, Fukuoka 812-8582, Japan*

Received 5 April 2004; accepted 26 April 2004

Abstract

Lung adenocarcinoma frequently has a histologic heterogeneity, particularly with regard to its cell morphology and growth pattern, with or without stromal desmoplasia. However, little is known about the relationship between morphologic heterogeneity and the destruction of BM. We selected 147 foci showing different growth patterns studied in 76 patients with lung adenocarcinoma and examined immunohistochemically the distribution of BM antigens, as well as the expression of MMPs and TIMP-2. BM antigens were more highly preserved in foci of the BAC growth pattern (94.7%) than in those of the papillary/acinar (24.5%) and solid patterns (16.1%) ($p<0.01$). MMP-2-positive cancer cells were significantly more frequent in poorly preserved foci of BM antigens than in preserved foci ($p<0.05$). The population of TIMP-2-positive cancer cells showed a positive correlation with BM preservation ($p<0.05$). However, no significant relationship between growth pattern and expression of MMP-9 and -14 was found. BM antigens had almost totally disappeared in desmoplastic foci. Multivariate analyses revealed that pathologic stage and high expression of TIMP-2 were independent prognostic factors. These findings indicate that the histologic heterogeneity of lung adenocarcinomas is partly related to the cancer cell–stromal interaction, in particular through BM preservation or destruction, which was mainly affected by cancer cell expression of MMP-2 and TIMP-2 in lung adenocarcinomas.
© 2004 Elsevier GmbH. All rights reserved.

Keywords: Histologic subtype; Stromal fibrosis; Immunohistochemistry; TIMP-2; MMP

Introduction

At the present time, lung cancer is one of the major cancers occurring worldwide [31], and adenocarcinoma is the most common type of lung cancer in western countries and Japan [33]. Lung adenocarcinomas frequently show histologic heterogeneity, particularly with regard to their growth pattern and cancer cell morphology. In the 1999 WHO classification [33], four

Abbreviations: The abbreviations used are: WHO, World Health Organization; BM, basement membrane; MMP, matrix metalloproteinase; TIMP, tissue inhibitor of metalloproteinase; BAC, bronchioloalveolar carcinoma

*Corresponding author. Tel.: +81-92-642-6060; fax: +81-92-642-5965.
E-mail address: sueishi@patholl.med.kyushu-u.ac.jp (K. Sueishi).

0344-0338/$ - see front matter © 2004 Elsevier GmbH. All rights reserved.
doi:10.1016/j.prp.2004.05.002

major subtypes were described: BAC, acinar, papillary, and solid adenocarcinoma, the majority of adenocarcinomas showing a mixture of the above histologic subtypes [11,33]. Adenocarcinoma is also frequently associated with stromal fibrosis caused by either desmoplasia or alveolar collapse, which is thought to be related to the chronologic progression of adenocarcinomas [26]. Recent studies suggest that the growth patterns and fibrosis correlate with the prognosis of adenocarcinoma patients [11,22].

The constituents of BM, composed mainly of laminin, type IV collagen, fibronectin, and other glycosaminoglycans, represent important determinants of cell differentiation, growth pattern, and other biologic functions of carcinoma cells because of respective receptor functions [2,17,23,24]. Therefore, the preservation or destruction of preexistent BM would be strongly affected by biologic properties of cancer cells, including growth pattern, stromal alterations such as desmoplasia and angiogenesis, and cancer cell invasiveness in the sense of a metastatic prerequisite. The architecture of interstitial matrices, including BM, is mainly modulated by the functional balance of degrading proteinases, MMPs, and their inhibitors, TIMPs. In tumor biology, in particular MMP-2, -9 and -14, and TIMP-1 and -2 have been investigated for their relationship to the malignant potential of cancer cells. In particular, overexpression of these MMPs by cancer cells has been suggested to reflect their invasiveness [1–3,6,15, 16,18,19,23,25,28]. Although the disruption of BM components seen in desmoplastic foci of non-BAC adenocarcinomas is closely associated with MMP-2 overexpression [10,23], little is known about the relationship between heterogeneous morphologies and the distributions of TIMPs and BM antigens in peripheral lung adenocarcinomas.

We used immunohistochemistry to examine the expression of MMP-2, -9, -14, and TIMP-2 in 147 foci of 76 primary lung adenocarcinomas, and compared the expression states with the growth patterns of the cancer cells by semiquantitatively assessing the degree of preservation of laminin and type IV collagen as major components of BM. In addition, we investigated the prognostic values of the histologic growth pattern, the expression of these MMPs and TIMP-2 of cancer cells, and the distribution pattern of BM, as well as other clinicopathologic variates.

Materials and methods

Seventy-six adenocarcinomas were obtained from 76 Japanese patients who had undergone, lobectomy or pneumonectomy at Kyushu University Hospital between 1992 and 1997. The pathologic stage was classified according to the tumor-node-metastasis staging system of the Union International Contre le Cancer [32] with minor modifications [30]. Clinicopathologic data of the patients are summarized in Table 1.

Histologic examination

The lungs were fixed with 10% neutral buffered formalin and embedded in paraffin. Four micrometer-thick sections were stained with elastica van Gieson (EVG) and Masson's trichrome stains to evaluate the type of fibrosis, and hematoxylin and eosin (HE) was used. The histopathologic diagnoses for whole

Table 1. Clinicopathologic data

	Histologic subtypes[a]			Total
	BAC	Papillary/acinar	Solid	
Age (years; mean ± SD)	47–79 (63.5 ± 12.9)	37–81 (66.4 ± 10.1)	51–82 (69.1 ± 8.0)	37–82 (66.9 ± 9.8)
Tumor size (mm; mean ± SD)	16–37 (26.3 ± 7.7)	9–90 (33.7 ± 15.6)	12–65 (36.0 ± 14.0)	9–90 (33.8 ± 14.7)
Gender				
Female	4	24	8	36
Male	2	25	13	40
Pathologic stage				
I	6	25	6	37
II–III	0	24	15	39
Lymph node metastasis				
Positive	0	18	11	29
Negative	6	31	10	47

BAC, bronchioloalveolar carcinoma.
[a] Histologic subtypes were based on WHO classification, 1999. Mixed types were transcribed with the major growth pattern.

Table 2. Relationship between histologic subtypes, growth patterns and fibrosis patterns

Histologic[a] subtypes	Case number (mixed type)	Number of foci					
		Growth pattern			Fibrosis pattern		
		BAC	Papillary/acinar	Solid	Collapse	Desmoplastic	
BAC	6(1)	6	0	0	0	1	7
Papillary/acinar	49(18)	10	49	10	9	21	99
Solid	21(6)	3	4	21	0	13	41
Total	76(25)	19	53	31	9	35	147

BAC, bronchioloalveolar carcinoma.
[a]Histologic subtypes were based on WHO classification, 1999. Mixed types were transcribed with the major growth pattern.

adenocarcinoma lesions were made on the basis of the 1999 WHO classification, with some modifications. Regarding the mixed subtypes, a predominant growth pattern was evident [11]. To assess the relationship between the growth pattern of cancer cells, with or without stromal fibrosis, and the distribution of BM constituents, we divided each adenocarcinoma lesion into 1–3 foci according to its growth pattern: (1) BAC, (2) papillary/acinar and (3) solid growth patterns (Table 2 and Figs. 1a–d), and fibrotic foci that were apparently delineated at low magnification (× 10), usually more than 5 mm in diameter (Table 2 and Figs. 1e–h). From findings of EVG and Mason's trichrome stainings, fibrotic foci were classified into two types on the basis of the criteria reported by Noguchi et al. [22]: (1) the collapse type (Figs. 1e and g), in which scar formation was predominantly due to alveolar collapse without apparent desmoplastic stromal reaction and (2) the desmoplastic type, in which scar formation was mainly attributable to a desmoplastic stromal reaction (Figs. 1f and h), i.e., fibrosis with significant fibroblastic proliferation.

Immunohistochemistry

Immunohistochemical examination was done for laminin, type IV collagen, MMP-2, -9, -14, and TIMP-2. Sections were deparaffinized and rehydrated. To retrieve respective antigenicity for laminin and type IV collagen, tissue sections were treated with 0.4% pepsin (Sigma, St. Louis, MO) in 0.1 N hydrochloride for 30 min at 37°C; for MMP-2, -9, and -14 and TIMP-2, sections were incubated in an autoclave for a few minutes at 121°C (0.01 mol/l citrate buffer, pH 6.0). After being washed in phosphate-buffered saline (PBS, pH 7.2, 0.01 mol/l) and treated with normal goat serum, sections were incubated at 4°C overnight with anti-human laminin rabbit polyclonal IgG (diluted to 1:25; Biogenex, San Roman, CA), anti-type IV collagen (3.0 μg/ml; DAKO, Glostrup, Denmark), MMP-2 (5.0 μg/ml; Fuji Chemical, Toyama, Japan), MMP-9 (2.5 μg/ml; Fuji Chemical), MMP-14 (30.0 μg/ml; Fuji Chemical), and TIMP-2 (5.0 μg/ml; Fuji Chemical). After having washed the sections in PBS and having treated them with 3% hydrogen peroxide in methanol for 15 min, we used the dextran polymer method (EnVision+TM, DAKO, Carpinteria, CA) for the detection of primary antibodies. Diaminobenzidine tetrahydrochloride was used as the chromogen, and sections were lightly counterstained with hematoxylin. Sections from breast carcinomas were used as positive controls for MMP-2 and TIMP-2. Normal lung tissue served as the internal positive control for laminin and type IV collagen, and infiltrating neutrophils were used for MMP-9. As negative controls, sections were similarly processed with preimmune rabbit or mouse serum instead of primary antibodies.

Semiquantitative assessment for the preservation of BM constituents and expression of MMPs and TIMP-2

The preservation of the BM constituents and the expressions of MMPs and TIMP-2 were evaluated separately for each growth pattern or fibrotic focus. The degree of BM preservation was assessed according to the method reported by Ohori et al. [23]. Briefly, when the immunoreactivity against both laminin and type IV collagen was preserved by more or less than 90% of length along the lepidic growth of cancer cells on alveolar surface or around neoplastic tubules, the BM pattern was categorized as A (Figs. 2a and b) or C (Figs. 2e and f), respectively. When at least one of the

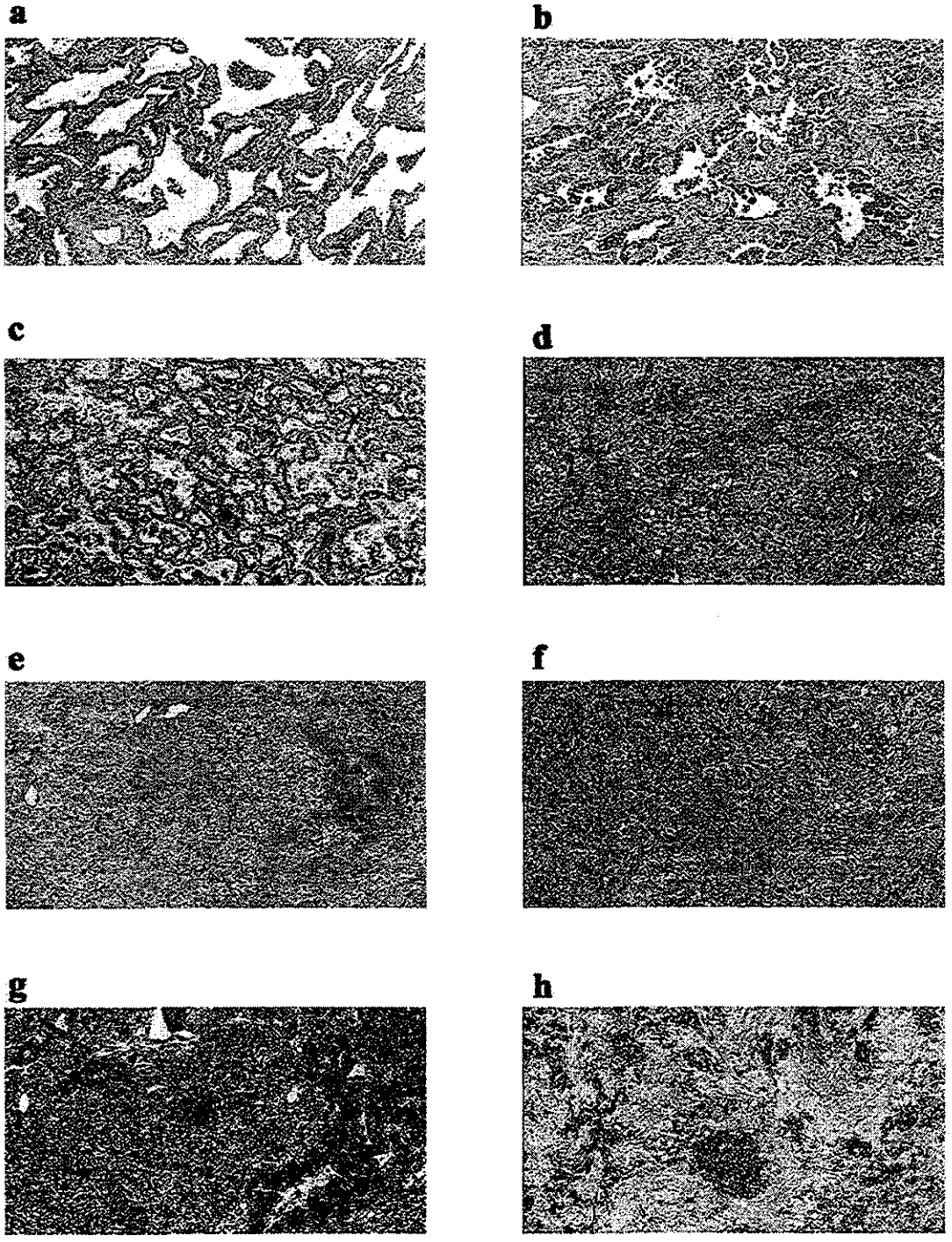

Fig. 1. Representative histologic findings of each growth pattern of cancer cells and fibrosis stroma pattern: (a) BAC type, (b) papillary, (c) acinar, and (d) solid growth pattern, and (e,g) collapse, and (f,h) desmoplastic fibrosis type, (a–f) HE, and (g and h) EVG staining, and original magnification: × 25.

BM components was preserved by over 90%, it was categorized as B (Figs. 2c and d).

To evaluate the expression of MMPs and TIMP-2 proteins, we counted the numbers of positive cells in more than 500 cancer cells and calculated respective positive cell ratios in each focus. As cancer cells had frequently disappeared in fibrotic foci, we excluded fibrotic foci from this evaluation.

The histologic subtyping and labeling indices of immunohistochemical parameters were independently determined by three blinded examiners (YM, TK, SH).